CELLULAR NEUROSCIENCE

Phagocytosis-driven neurodegeneration through opposing roles of an ABC transporter in neurons and phagocytes

Xinchen Chen, Bei Wang, Ankita Sarkar†, Zixian Huang‡, Nicolas Vergara Ruiz, Ann T. Yeung§, Rachael Chen¶, Chun Han*

Copyright © 2025 The Authors, some rights reserved; exclusive licensee American Association for the Advancement of Science. No claim to original U.S. Government Works. Distributed under a Creative Commons Attribution NonCommercial License 4.0 (CC BY-NC).

Lipid homeostasis is critical to neuronal survival. ATP-binding cassette A (ABCA) proteins are lipid transporters associated with neurodegenerative diseases. How ABCA transporters regulate lipid homeostasis in neurodegeneration is an outstanding question. Here we report that the *Drosophila* ABCA protein engulfment ABC transporter in the ovary (Eato) regulates phagocytosis-dependent neurodegeneration by playing opposing roles in neurons and phagocytes: In neurons, Eato prevents dendrites and axons from being attacked by neighboring phagocytes; in phagocytes, Eato sensitizes the cell for detecting neurons as engulfment targets. Thus, *Eato* deficiency in neurons alone causes phagocytosis-dependent neurite degeneration, but additional *Eato* loss from phagocytes suppresses the neurite degeneration. Mechanistically, Eato functions by removing the eat-me signal phosphatidylserine from the cell surface in both neurons and phagocytes. Multiple human and worm ABCA homologs can rescue *Eato* loss in phagocytes but not in neurons, suggesting both conserved and cell type–specific activities of ABCA proteins. These results imply possible mechanisms of neuron-phagocyte interactions in neurodegenerative diseases.

INTRODUCTION

For a neuron to survive and function, the composition and spatial distribution of its lipids need to be dynamically maintained within a narrow range of optimal levels. Lipid homeostasis is controlled largely by lipid transporters located on cell membranes. ATP-binding cassette (ABC) proteins comprise a large family of transporters that contain conserved nucleotide-binding domains and that translocate diverse substrates across cell membranes using energy from adenosine triphosphate (ATP) (*1*, *2*). Among ABC proteins, the ABCA subfamily is best known for its functions in transporting lipids across the bilayer and loading lipids onto apolipoprotein carriers (*2*–*4*). The importance of ABCA genes in human health is underscored by numerous mutations that are associated with diverse inheritable diseases related to lipid transport, including multiple neurodegenerative diseases (*4*–*6*).

Several ABCA proteins in humans and other animals are protective of neurons. Genome-wide association studies identified *ABCA1* and *ABCA7* as risk genes for Alzheimer's disease (AD) (*7*, *8*). In mice, ABCA1 promotes the efflux of excess cholesterols from the brain and the lipidation of apolipoproteins, including the AD-associated ApoE (*9*–*11*). High membrane cholesterol promotes production of the neurotoxic amyloid-β peptide (Aβ) (*12*, *13*), while lipidated ApoE can bind Aβ and is negatively correlated with AD (*14*, *15*). ABCA7 reduces Aβ production by affecting amyloid precursor protein (APP) processing (*16*, *17*) and can also reduce the buildup of extracellular Aβ by promoting phagocytosis (*18*, *19*). Unlike most ABCA proteins, which act as floppases to export lipids from the cytosolic to the extracellular leaflet of the plasma membrane, the Stargardt disease-associated ABCA4 protein is a flippase responsible for importing retinoids into rod photoreceptors and retinal pigment epithelial cells (*20*–*22*). Thus, mutations in *ABCA4* result in accumulation of toxic retinoids and subsequent photoreceptor degeneration. In *Drosophila*, two ABCA proteins, Engulfment ABC transporter in the ovary (Eato) and Lipid droplet defective (Ldd), export toxic lipids induced by oxidative stress from photoreceptors to nearby glia (*23*, *24*). Consequently, the loss of *Eato* or *ldd* results in early photoreceptor degeneration in the presence of oxidative stress (*24*). Despite these advances, whether ABCA proteins are involved in neurodegeneration through other means remains to be explored.

Besides their structural roles in membranes, lipids can also contribute to neurodegeneration through signaling functions. Phosphatidylserine (PS) is a phospholipid normally found in the inner leaflet of the plasma membrane (*25*). However, in sick or degenerating neurons, PS translocates to the extracellular leaflet, where it functions as a cell surface "eat-me" signal to induce phagocytosis of neurites by nearby phagocytes (*26*). PS-induced phagocytosis not only enables clearance of neuronal debris resulting from degeneration but can also potently break down neurites of live neurons (*27*, *28*). The asymmetric distribution of PS on the plasma membrane of healthy cells is established and maintained by flippases that belong to the P4–adenosine triphosphatase (ATPase) family of lipid transporters (*25*, *29*). On the other hand, lipid scramblases in the TMEM16 and XK-related families disrupt PS asymmetry and are responsible for PS exposure on platelets and apoptotic cells, respectively (*30*–*32*).

Among ABCA proteins, murine ABCA1 was first found to promote Ca^{2+}-induced PS exposure at the plasma membrane (*33*). Similarly, a *Caenorhabditis elegans* ABCA protein, Cell death abnormal 7 (CED-7), was later discovered to facilitate PS exposure on apoptotic cells in the developing embryo and the subsequent transfer of PS-exposing extracellular vesicles from apoptotic cells to phagocytes (*34*–*36*). These observations are consistent with most ABCA proteins

Weill Institute for Cell and Molecular Biology, Department of Molecular Biology and Genetics, Cornell University, Ithaca, NY 14853, USA.
*Corresponding author. Email: chun.han@cornell.edu
†Present address: NovaSterilis Inc., Lansing, NY 14882, USA.
‡Present address: Department of Developmental Biology, Washington University School of Medicine, Saint Louis, MO 63110, USA.
§Present address: Harvard Medical School, Boston, MA 02115, USA.
¶Present address: School of Medicine and Dentistry, University of Rochester, Rochester, NY 14642, USA.

being lipid floppases (*2*, *37*), and their ability to promote PS exposure has been thought to be important for the functions of ABCA proteins in phagocytosis (*33*). To date, it remains unknown how ABCA proteins may participate in neurodegeneration by regulating PS transport.

In this study, we show that the *Drosophila* ABCA protein Eato regulates phagocytosis-driven dendrite and axon degeneration by playing opposing roles in neurons and phagocytes: In neurons, it prevents dendrites and axons from being engulfed by phagocytes; in phagocytes, instead of being required for phagocytosis, it makes the cell more sensitive to PS presented by nearby engulfment targets. Thus, although the loss of *Eato* in neurons alone results in degeneration of diverse neurons in both the peripheral nervous system (PNS) and central nervous system (CNS), removing *Eato* in both neurons and phagocytes rescues neuronal degeneration. Despite these two distinct cell type–specific roles for Eato, unexpectedly, it functions in both neurons and phagocytes by suppressing, rather than enhancing, the effects of PS on cell surface. In support of Eato's function in phagocytes, we further found that PS exposure on phagocytes inhibits, instead of promoting, phagocytosis. Last, we show that CED-7 and several mammalian ABCA homologs can partially compensate for the loss of *Eato* in phagocytes but not in neurons, suggesting both conserved and cell type–specific functions of ABCA proteins in regulating lipid homeostasis and phagocytosis-dependent neurodegeneration.

RESULTS

Eato LOF in da neurons causes engulfment-dependent dendrite degeneration

To search for lipid transporters that may affect exposure of eat-me signals on the plasma membrane of neurons, we screened candidate genes in the ABCA subfamily by RNA interference (RNAi) and CRISPR-induced mutagenesis (*38*) in *Drosophila* class IV dendritic arborization (C4da) neurons. C4da neurons are somatosensory neurons that grow highly elaborated dendrites underneath epidermal cells on the larval body wall (*39*); these neurons are a well-established model system for studying degeneration and phagocytosis of dendrites (*27*, *28*, *40*, *41*). Among the genes we examined, only the loss of function (LOF) of *Eato* led to dendrite degeneration. In these assays, C4da neurons were labeled by membrane-associated pH sensor (MApHS), a dual fluorescent membrane marker that contains both a pH-sensitive pHluorin and an acid-resistant tdTomato (tdTom) (*40*). Degenerating dendrites are engulfed by larval epidermal cells, resulting in tdTom-labeled neuronal debris inside phagosomes that are dispersed in epidermal cells (*40*). To knock out *Eato* in C4da neurons, we combined the C4da-specific *ppk-Cas9* (*38*) with *gRNA-Eato*, which expresses ubiquitously two guide RNAs (gRNAs) targeting the shared coding sequence of both *Eato* splicing variants (Fig. 1A). Compared to control neurons that showed no debris (Fig. 1, B and G), *Eato* knockout (KO) neurons exhibited a 70.8% reduction in dendrite length along with widespread dendrite debris in the epidermis at 96 hours after egg laying (AEL), indicating severe degeneration (Fig. 1, C, F, and G). This phenotype was further confirmed by C4da-specific *Eato* knockdown (KD) with a short hairpin RNA transgene (HMC06027) targeting the shared coding sequence of *Eato* (Fig. 1, A and D to G). To understand how this degeneration phenotype develops, we examined *Eato* KO neurons at multiple developmental stages from 48 hours AEL to 120 hours AEL. *Eato* KO neurons did not show obvious signs of degeneration at 48 hours AEL but displayed substantial debris and gradually more severe dendrite reduction from 72 hours AEL onward (Fig. 1, H to M), demonstrating a progressive loss of dendrites due to degeneration.

Degenerating neurons display the eat-me signal PS on their surface, which triggers phagocytic clearance of neuronal debris by phagocytes (*27*). Considering that *Eato* encodes a putative ABCA lipid transporter, we wondered whether *Eato* KO neurons display PS exposure. We previously developed an in vivo extracellular PS labeling system in which PS binding probes fused to fluorescent proteins, such as green fluorescent protein GFP-Lactadherin C1C2 domains (GFP-Lact), are expressed by the fat body and secreted into the larval body fluid (*27*). Peripheral tissues with surface PS exposure are coated by the probes. Using GFP-Lact, we detected strong PS externalization on the dendrites of *Eato* KO neurons but not on control neurons (Fig. 1, N to O"), consistent with the degenerating state of these KO neurons.

We previously found that PS exposure on neuronal surfaces can induce neurite degeneration (*27*, *28*). In such a scenario, phagocytes engulf PS-exposing (but intact and living) neurites, and the phagocytosis is responsible for the neurite degeneration. However, the observation of PS exposure on *Eato* KO neurons does not necessarily indicate that phagocytosis causes the degeneration, considering that PS exposure could be a consequence of membrane disruptions expected of dendrite degeneration (*27*). To determine whether the dendrite degeneration associated with *Eato* LOF depends on phagocytosis, we knocked out *Eato* in a null mutant of *draper* (*drpr*), which encodes an engulfment receptor required for larval epidermal cells to phagocytose degenerating dendrites (*40*). Notably, dendrite degeneration of *Eato* KO neurons was completely suppressed in the *drpr* mutant (Fig. 1, P to T). These data show that dendrite degeneration of *Eato* deficient neurons is caused by the phagocytic activity of epidermal cells.

Eato LOF makes epidermal cells insensitive to degenerating dendrites

To further investigate the LOF phenotype of *Eato*, we generated an *Eato* CRISPR mutant by knocking out *Eato* in the germ line. $Eato^{10}$ contains a deletion of 709 nucleotides from exon 4 to exon 6 between the two gRNA target sites (Fig. 1A), resulting in a reading frame shift from amino acid 201 and thus is expected to be a null allele. Unexpectedly, when examining C4da neurons in heterozygotes of $Eato^{10}$ and *Df(BSC812)*, a deficiency lacking the entire *Eato* locus, we did not observe any signs of dendrite degeneration (Fig. 2, B, E, and F), a sharp contrast with the C4da-specific KO of *Eato* (Fig. 2, A, E, and F). *Eato* was previously shown to be involved in phagocytosis of nursing cells by follicular epithelial cells during *Drosophila* oogenesis (*42*), and ABCA homologs in worms (CED-7) and mammals (ABCA1) participate in phagocytosis as well (*33*, *35*). Given the requirement of phagocytosis for the dendrite degeneration of *Eato*-deficient neurons (Fig. 1, P to T), we hypothesized that epidermal cells require *Eato* to engulf *Eato*-deficient dendrites. To test this idea, we knocked down *Eato* simultaneously in both neurons and epidermal cells. This led to a wild-type (WT) dendrite phenotype (Fig. 2, D to F), as compared to the severe degeneration seen in neuron-specific KD (Fig. 2, C, E, and F), confirming a requirement for *Eato* in the phagocytic destruction of *Eato* mutant neurons by epidermal cells.

Eato could be required for epidermal cells to engulf *Eato*-deficient neurons specifically or to engulf any neuron displaying eat-me signals.

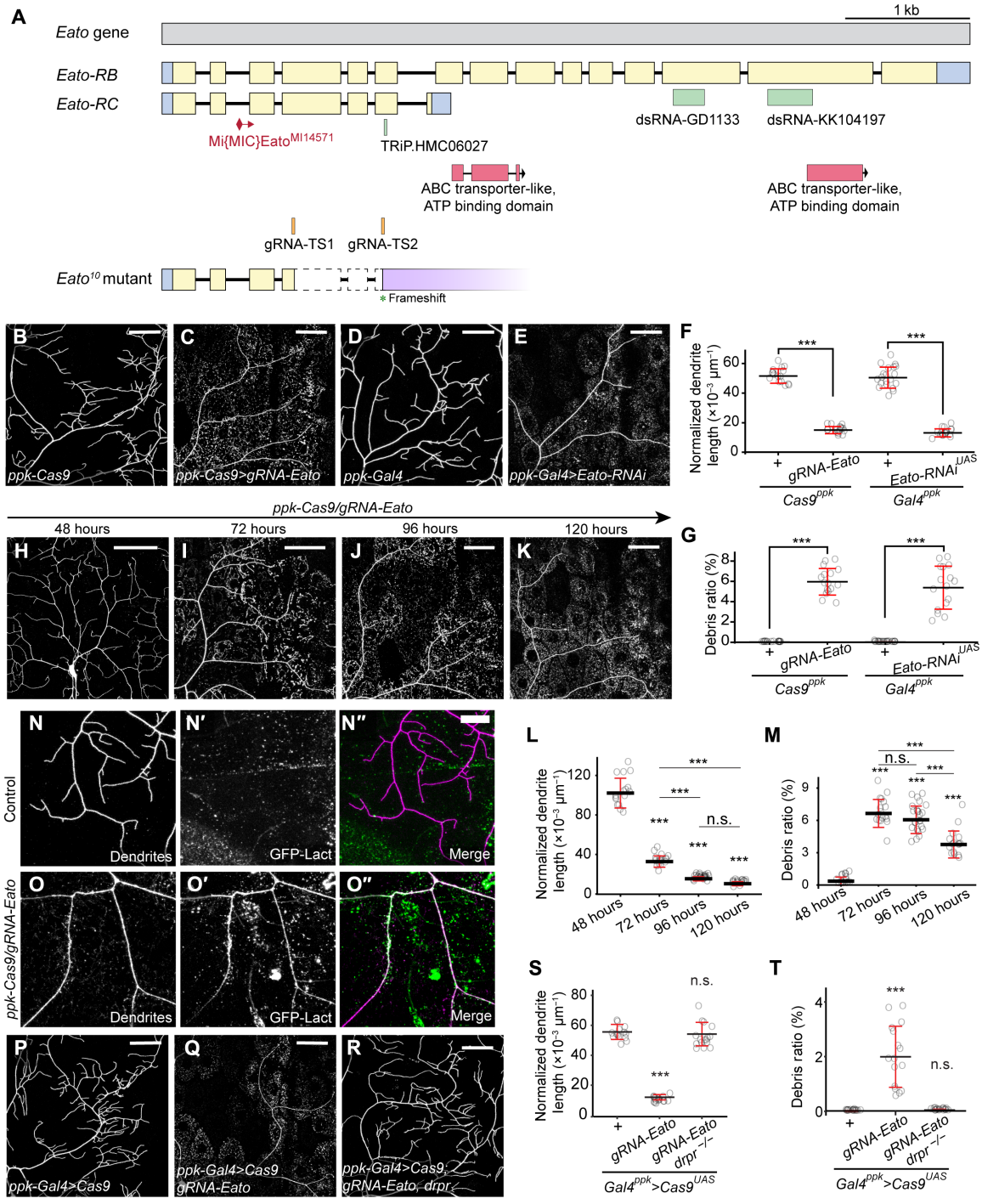

Fig. 1. *Eato* LOF in C4da neurons leads to engulfment-dependent dendrite degeneration. (**A**) *Eato* gene structure and reagents used in this study. (**B** to **E**) C4da neuron dendrites in *ppk-Cas9* control (B), C4da-specific *Eato* KO (C), *ppk-Gal4* control (D), and C4da-specific *Eato* KD (E). (**F** and **G**) Normalized dendrite length (total dendrite length/total area) (F) and debris ratio (debris area/total area) (G) in (B) to (E). *n* = neuron number and *N* = animal number: $Cas9^{ppk}$ (*n* = 16, *N* = 9); $Cas9^{ppk}$ *gRNA-Eato* (*n* = 16, *N* = 8); $Gal4^{ppk}$ (*n* = 20, *N* = 11); $Gal4^{ppk}$>*Eato-RNAi* (*n* = 16, *N* = 14). (**H** to **K**) Dendrites of C4da-specific *Eato* KO across different developmental stages. (**L** and **M**) Normalized dendrite length (L) and debris ratio (M) in (H) to (K). Sample sizes: 48 hours (*n* = 16, *N* = 8); 72 hours (*n* = 17, *N* = 11); 96 hours (*n* = 24, *N* = 12); 120 hours (*n* = 16, *N* = 8). (**N** to **O**″) Binding patterns of the PS sensor GFP-Lact on control [(N) to (N″)] and *Eato* KO neurons [(O) to (O″)]. Fat body–specific *dcg-Gal4* drives expression of GFP-Lact. (**P** to **R**) C4da neuron dendrites in *ppk-Gal4 UAS-Cas9* control (P), C4da-specific *Eato* KO (Q), and C4da-specific *Eato* KO in $drpr^{indel3}$ homozygous mutant (R). (**S** and **T**) Normalized dendrite length (S) and debris ratio (T) in (P) to (R). Sample sizes: $Gal4^{ppk}$>$Cas9^{ppk}$ (*n* = 15, *N* = 10); $Gal4^{ppk}$>*Cas9 gRNA-Eato* (*n* = 16, *N* = 11); $Gal4^{ppk}$>*Cas9 gRNA-Eato* $drpr^{indel3}$ (*n* = 16, *N* = 12). C4da neurons were labeled by *ppk-MApHS* in (B) to (E) and (H) to (K), *ppk-CD4-tdTomato* in (N) to (O″), and *ppk-Gal4 UAS-CD4-tdTomato* in (P) to (R). Scale bars: 50 μm [(B) to (E), (H) to (K), and (P) to (R)] and 20 μm [(N) to (O″)]. ***$P < 0.001$; n.s., not significant; one-way analysis of variance (ANOVA) with Tukey post hoc test.

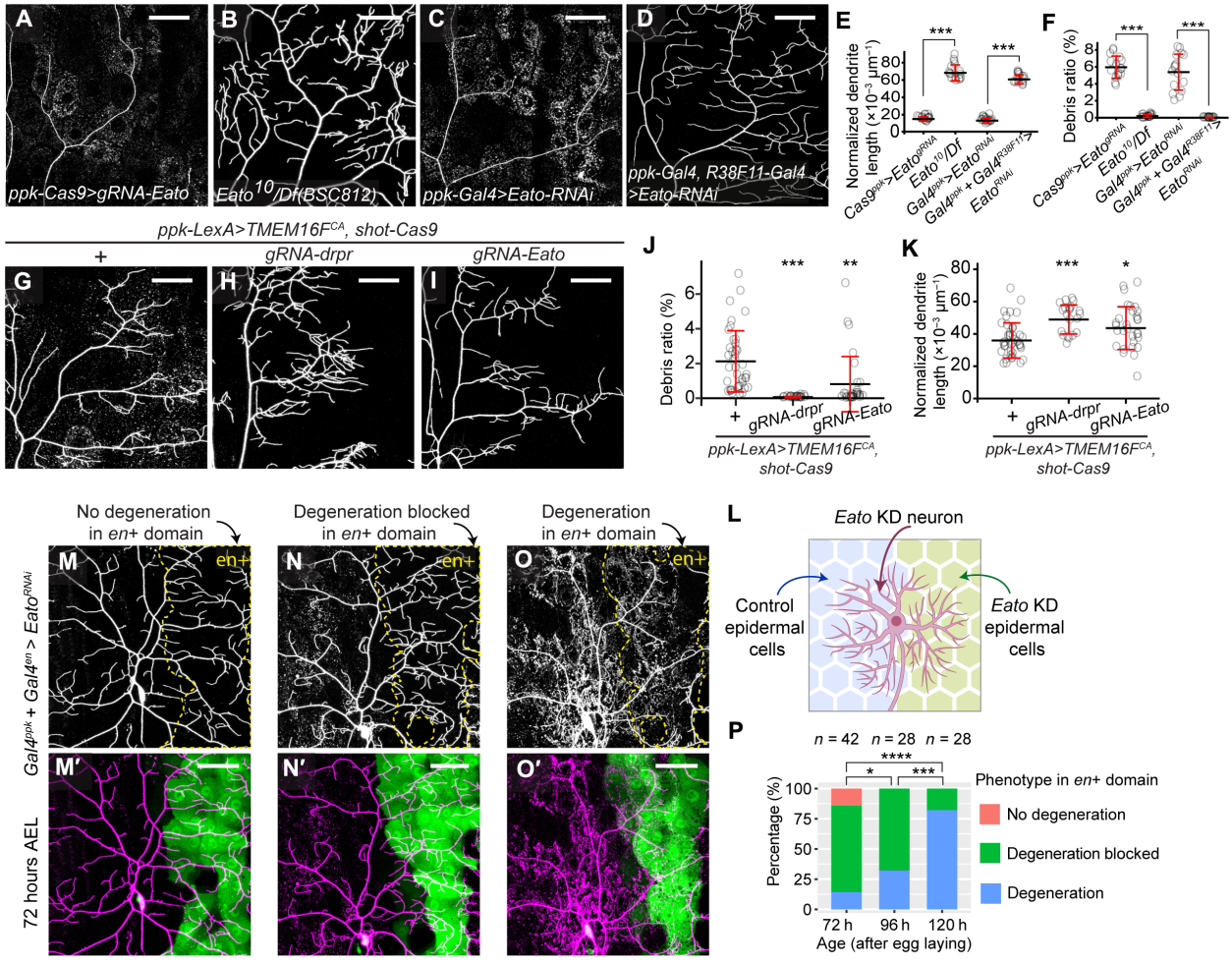

Fig. 2. *Eato* LOF makes epidermal cells insensitive to degenerating dendrites. (**A** to **D**) C4da neuron dendrites in C4da-specific *Eato* KO (A), $Eato^{10}/Df(BSC812)$ transheterozygous mutant (B), C4da-specific *Eato* KD (C), and both C4da and epidermal cell–specific *Eato* KD (D). (**E** and **F**) Normalized dendrite length (E) and debris ratio (F) in (A) to (D). Sample sizes: $Cas9^{ppk}>Eato^{gRNA}$ ($n = 16$, $N = 8$); $Eato^{10}/Df$ ($n = 16$, $N = 7$); $Gal4^{ppk}>Eato^{RNAi}$ ($n = 16$, $N = 14$); $Gal4^{ppk} + Gal4^{R38F11}>Eato^{RNAi}$ ($n = 16$, $N = 9$). (**G** to **I**) C4da neuron dendrites of $TMEM16F^{CA}$-overexpressing (OE) C4da neurons with control epidermal cells (G), epidermal cell–specific *drpr* KO (H), and epidermal cell-specific *Eato* KO (I) in late third-instar larvae. (**J** and **K**) Quantification of normalized dendrite length (J) and debris ratio (K) in (G) to (I). Sample sizes: *ppk-LexA>TMEM16F^{CA} shot-Cas9* ($n = 40$, $N = 19$); *ppk-LexA>TMEM16F^{CA} shot-Cas9 gRNA-drpr* ($n = 21$, $N = 15$); *ppk-LexA>TMEM16F^{CA} shot-Cas9 gRNA-Eato* ($n = 30$, $N = 15$). (**L**) Experiment design in (M) to (O′). (**M** to **O′**) C4da neuron dendrites from the experiment described in (L). *en+* domains in grayscale images are enclosed by yellow dashed lines. Three categories of phenotypes: no degeneration [(M) and (M′)], degeneration blocked in the *en+* domain [(N) and (N′)], and degeneration in *en+* domain [(O) and (O′)]. (**P**) Percentage of three genotypes in 72 to 120 hours (h) AEL animals. Sample sizes: 72 hours ($n = 42$, $N = 18$); 96 hours ($n = 28$, $N = 14$); 120 hours ($n = 28$, $N = 14$). Pan-epidermal expression is driven *R38F11-Gal4*. Pan-epidermal KO is driven by *shot-Cas9*. C4da neurons were labeled by *ppk-MApHS* in (A) to (D), (G) to (I), and (M) to (O′). Scale bars, 50 μm. $^*P < 0.05$, $^{**}P < 0.01$, $^{***}P < 0.001$, and $^{****}P < 0.0001$; [(E), (F), (J), and (K)] one-way ANOVA with Tukey post hoc test; (P) chi-square test, *P* value adjusted by a false discovery rate method.

To distinguish between these two possibilities, we sought to induce ectopic PS exposure on dendrites using the murine TMEM16F, a calcium-dependent phospholipid scramblase whose activity results in externalization of PS on the plasma membrane (*30*). Because expression of TMEM16F in C4da neurons causes only weak PS exposure (*27*), to induce stronger PS exposure on dendrites, we expressed a constitutively active TMEM16F mutant ($TMEM16F^{CA}$) carrying two mutations (Y563K/D703R) that make the scramblase calcium independent (*43*). As expected, $TMEM16F^{CA}$ expression resulted in a moderate level of dendrite debris in epidermal cells (Fig. 2, G and J). The dendrite debris was completely eliminated, however, when *drpr* was simultaneously knocked out from epidermal cells using tissue-specific CRISPR (Fig. 2, H and J) (*38*), confirming the dependence of this dendrite degeneration on phagocytosis. Epidermal-specific *Eato* KO also suppressed the dendrite debris of $TMEM16F^{CA}$-expressing neurons and increased the dendrite length (Fig. 2, I to K), although in either case not as potently as *drpr* KO. These results suggest that *Eato* LOF in epidermal cells impairs the ability of these cells to engulf PS-exposing dendrites.

Eato may be absolutely required for phagocytosis or only enhance the ability of epidermal cells to engulf, two possibilities that can potentially be distinguished by presenting *Eato*-deficient epidermal cells with engulfment targets of higher PS exposure. We previously showed that dendrites physically severed from the cell body exhibit a burst of high PS exposure before they segment (*27*, *28*),

leading to efficient engulfment and clearance of the dendrites (fig. S1, A and D). The engulfment of such injured dendrites is blocked in *drpr* mutants (*28*, *40*): In the absence of engulfment, fragmented dendrite pieces still lined up in the original branching pattern 20 hours after injury (fig. S1B). In contrast, injured dendrites were completely engulfed by *Eato*-KD epidermal cells, as reflected by the dendrite debris widely spread in epidermal cells (fig. S1, C to E). These data suggest that *Eato* is not required for phagocytosis per se; rather, it is needed for epidermal cells to detect moderate levels of PS exposure on dendrites, such as in TMEM16F^{CA} expression.

To further confirm that Eato only enhances phagocyte sensitivity but is not required for engulfment, we exposed *Eato*-deficient neurons (via KD) to both WT and *Eato*-deficient epidermal cells in the same animal. The WT control epidermal cells are in the anterior half of each segment, while *Eato* KD is induced in the posterior half of the segment by *en-Gal4* (Fig. 2L). We reasoned that the anterior WT epidermal cells should attack *Eato*-deficient neurons and cause dendrite injury. If the injury signals spread to posterior dendrites, these dendrites may show elevated levels of eat-me signals and thus allow us to test the ability of *Eato*-deficient posterior epidermal cells to engulf them. In third-instar animals, we observed three classes of phenotypes: (i) a "no degeneration" phenotype, in which neither the control domain (anterior) nor the *en+* domain (posterior) showed dendrite degeneration (Fig. 2, M and M′); (ii) a "blocked degeneration" phenotype, in which only the control but not the *en+* domain showed dendrite degeneration (Fig. 2, N and N′); and (iii) a "degeneration" phenotype, in which both the control and the *en+* domain showed dendrite degeneration (Fig. 2, O and O′). At 72 hours AEL, most neurons (71.4%) showed blocked degeneration, and only small fractions showed no degeneration (14.3%) or degeneration (14.3%) (Fig. 2P), suggesting that posterior dendrites are locally protected due to *Eato* LOF in posterior epidermal cells. However, the degeneration phenotype increased to 32.1% at 96 hours AEL and 82.1% at 120 hours AEL (Fig. 2P). These observations are consistent with the idea that posterior dendrites become increasingly sick with age and are eventually recognized and engulfed by *Eato*-deficient epidermal cells. Thus, *Eato* is not necessary for phagocytosis in epidermal cells, but the loss of *Eato* reduces the sensitivity of epidermal cells to mildly unhealthy dendrites and delays the initiation of phagocytosis.

Eato LOF in da neurons causes glia-dependent axon degeneration

Like dendrites, axons exhibit PS-induced engulfment and degeneration (*27*, *44*, *45*). However, axons and dendrites differ in their requirements for specific components of the axon-death pathway in injury-induced degeneration (*28*). We thus tested whether *Eato* is also required to maintain the integrity of C4da axons, which project to the ventral nerve cord (VNC) in a ladder pattern (Fig. 3A). When *Eato* was knocked out from C4da neurons, the axon ladder became fragmented (Fig. 3, B and D), indicating axon degeneration. Like dendrite degeneration, this axon degeneration was also completely suppressed in the *drpr* mutant (Fig. 3, C and D), demonstrating that phagocytosis also drives axon degeneration of *Eato*-deficient neurons.

In the CNS, glia are the phagocytes that engulf dead neurons and neuronal debris (*26*, *46*). The axons of dendritic arborization (da) neurons are surrounded by glia in both peripheral nerves and the VNC. Hence, we asked whether glia are involved in axon degeneration of *Eato*-deficient neurons by knocking down *Eato* in both C4da neurons and glia. Unlike C4da-specific *Eato* KD, which showed marked axon degeneration (Fig. 3, E and H), *Eato* KD in both neurons and glia showed no axon degeneration (Fig. 3, F and H). These data confirm that glia are required for the phagocytosis-dependent axon degeneration and further demonstrate that *Eato* promotes phagocytic activity of glia.

Although the dendritic and axonal compartments of the same da neuron are attacked by different phagocyte types, we wondered whether degeneration of the two compartments is coupled. We thus knocked down *Eato* in both neurons and epidermal cells to suppress dendrite degeneration (fig. S2, A, C, E, and F) and examined axon morphology. These neurons showed much weaker axon degeneration than neuronal KD alone (Fig. 3, E, G, and H). In contrast, knocking down *Eato* in both neurons and glia to suppress axon degeneration had no impact on dendrite degeneration (fig. S2, D and F). These data together suggest that damage to dendrites strongly enhances phagocytosis of axons, likely by promoting exposure of eat-me signals on axons, but axon degeneration is compartmentally restricted and does not affect dendrites in the same neuron.

Eato encodes a membrane protein required for the integrity of diverse neurons in both the PNS and CNS

To determine where else *Eato* may play a role in protecting neurons from degeneration, we first examined Eato expression patterns by generating an *Eato-Gal4* transcription reporter. *MiMIC*^{MI14571} (*47*) is a transgenic insertion in the second intron, which is between two coding exons shared by both *Eato* isoforms (Fig. 1A). We converted *MiMIC*^{MI14571} to a *2A-Gal4* Trojan exon through recombinase-mediated cassette exchange (fig. S3A) (*48*). The resultant *Eato-Gal4* should produce a short truncated Eato protein (102 amino acids) and a Gal4 driven by the endogenous regulatory sequence of *Eato* that should recapitulate the *Eato* expression pattern. By crossing to UAS-driven fluorescent reporters, we observed broad *Eato-Gal4* expression in peripheral tissues, including da neurons, bipolar dendrite (bd) neurons, a subset of external sensory (es) neurons, epidermal cells (Fig. 4, A to A"), peripheral glia (Fig. 4, B to B"), muscles (fig. S3, B and C), and the trachea (fig. S3D). In the VNC, *Eato-Gal4* expression overlaps with some but not all neurons and glia (Fig. 4, C to D").

Next, we asked where the Eato protein is localized in cells. First, we generated a FLAG-tagged *UAS-Eato* (the long isoform B) transgene and expressed it in epidermal cells. FLAG staining was detected strongly on the lateral plasma membrane, overlapping with the membrane marker Nrg-GFP, and also at lower levels in intracellular vesicles (Fig. 4, E and E′). Next, to determine the localization of endogenous Eato proteins in epidermal cells and neurons, we inserted a [*mNeonGreen11* (*mNG$_{11}$*)*–OLLAS*]×*4-2A-QF2* [OLLAS (*Escherichia coli* OmpF Linker and mouse Langerin fusion Sequence)] cassette in the *Eato* locus immediately before the stop codon of the longer isoform (fig. S3E) using a gRNA-donor vector optimized for CRISPR activity in the *Drosophila* germ line (*49*). mNG$_{11}$ is a fragment of split mNG and can reconstitute the full fluorescent mNG protein when mNG$_{1–10}$ is coexpressed in the same cell (*50*). OLLAS is a short tag, for which high-affinity antibodies are available (*51*). *2A-QF2* in the construct allows identification of knock-in (KI) candidates by crossing to *QUAS*-driven fluorescent reporters (*52*). mNG$_{11}$ enables detection of Eato proteins in specific cells, while OLLAS staining can visualize Eato proteins in all expressing tissues. Using OLLAS staining, we confirmed the presence of Eato on the plasma membrane and intracellular vesicles of epidermal cells (stars in Fig. 4F)

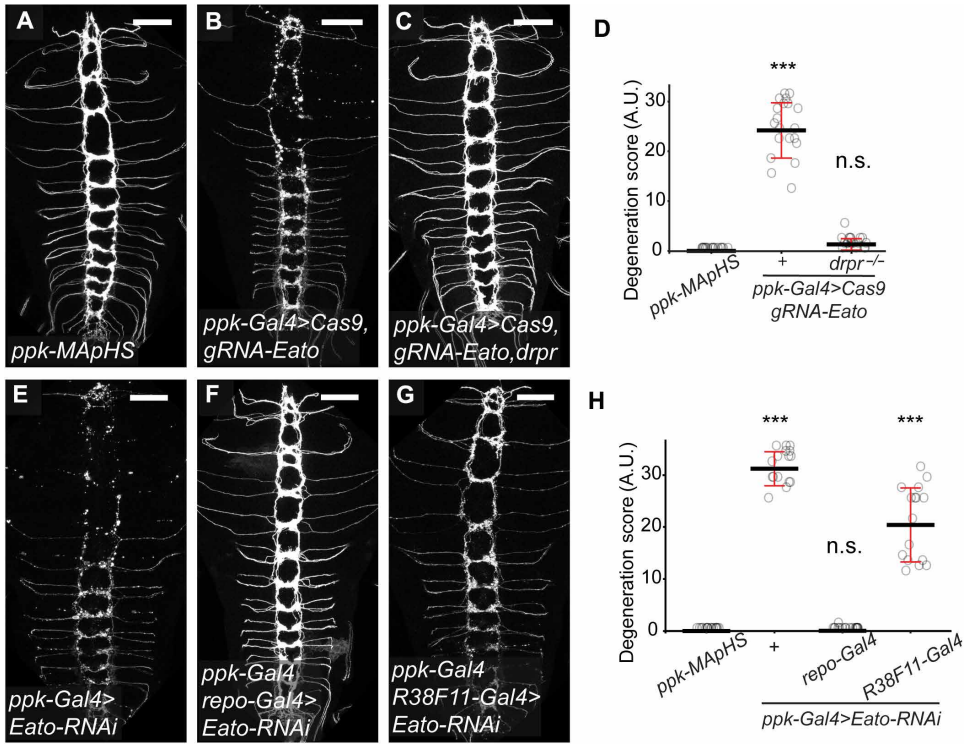

Fig. 3. *Eato* LOF in da neurons causes glia-dependent axon degeneration. (**A** to **D**) Axons of C4da neurons in *ppk-Gal4 UAS-Cas9* control (A), C4da-specific *Eato* KO (B), and C4da-specific *Eato* KO in $drpr^{indel3}$ homozygous mutant (C) late third-instar larvae. Degeneration level is quantified as degeneration score in (D) (see Materials and Methods). *n* = number of brains: *ppk-MApHS* (*n* = 16); *ppk-Gal4>Cas9 gRNA-Eato* (*n* = 21); *ppk-Gal4>Cas9 gRNA-Eato* $drpr^{-/-}$ (*n* = 19). (**E** to **H**) Axons of C4da neurons in C4da-specific *Eato* KD (E), C4da and glia-specific *Eato* KD (F), and C4da and epidermal cell-specific *Eato* KD (G) animals. Degeneration level is quantified as degeneration score in (H). *n* = number of brains: *ppk-MApHS* (*n* = 16); *ppk-Gal4>Eato-RNAi* (*n* = 17); *ppk-Gal4* + *repo-Gal4>Eato-RNAi* (*n* = 18), *ppk-Gal4* + *R38F11-Gal4>Eato-RNAi* (*n* = 16). Glia-specific expression is driven by *repo-Gal4*. C4da neurons were labeled by *ppk-MApHS* in (A) to (C) and (E) to (G). Scale bars, 50 μm. In all plots, ***$P < 0.001$; n.s., not significant, one-way ANOVA with Tukey post hoc test. A.U., arbitrary units.

and detected signals that appeared as dendritic patterns of sensory neurons (arrowheads in Fig. 4F). By expressing $mNG_{1–10}$ using a pan-neuronal Gal4 (*RabX4-Gal4*), we detected reconstituted mNG signals on the soma, axons, and dendrites of da neurons (Fig. 4G). mNG fluorescence appeared as smooth signals on the neuronal surface and also in bright puncta resembling intracellular vesicles.

The broad expression of *Eato* in the nervous system prompts the question of whether *Eato* is also important in neurons other than C4da. To answer this question, we generated MApHS-labeled $Eato^{10}$ homozygous mutant clones in both the PNS and the CNS of otherwise $Eato^{10/+}$ heterozygous animals using a technique called mosaic analysis by gRNA-induced crossing-over (MAGIC) (*53*). $Eato^{10}$ clones of class I to III da neurons showed severe dendritic degeneration as indicated by reduced dendrites and extensive neuronal debris near dendrites (Fig. 4, H and I, and fig. S3F). Mutant multidendritic dmd1 neurons also showed debris near dendrites (fig. S3G). We did not observe obvious degeneration at axon terminals of motor neurons (fig. S3H). In the larval VNC (fig. S3, I and J), the larval brain (fig. S3, K and L), adult optical lobe (Fig. 4, J and K), and central brain (fig. S3, M and N), $Eato^{10}$ mutant neurons showed severely fragmented neurites with blebbing, contrasting with the smooth and continuous signals on WT neuronal clones. These data show that *Eato* is required to maintain the integrity of a broad range of neurons. Consistent with this conclusion, pan-neuronal *Eato* KD using *RabX4-Gal4* caused pupal lethality. Considering that homozygous *Eato* mutant strains are viable and fertile, degeneration of *Eato* homozygous mutant neurons in otherwise heterozygous animals is most likely caused by *Eato*-dependent engulfment activity of resident phagocytes in the PNS and CNS, as is the case for C4da neurons (Fig. 2D).

Putative ABCA transporter activity is required for Eato's function

The *Eato* locus produces two alternatively spliced transcripts of different lengths (Fig. 1A): The longer *Eato-RB* isoform encodes a full-length ABCA protein, with two ABC transporter-like ATP-binding domains (InterPro IPR003439), while the shorter *Eato-RC* isoform ends before the first ABC transporter-like domain. To determine whether the full-length isoform is responsible for Eato's function in neurons and phagocytes, we knocked down *Eato* using two additional RNAi lines (GD1133 and KK104197) that target *Eato-RB* only (Fig. 1A). Expression of $Eato\text{-}RNAi^{KK104197}$ in C4da neurons with *ppk-Gal4* caused strong dendrite degeneration, albeit slightly weaker than that with $Eato\text{-}RNAi^{HMC06027}$, which targets both isoforms (Fig. 5, A to E). When driven by $Gal4^{21\text{-}7}$, an early pan-da driver (*54*), $Eato\text{-}RNAi^{GD1133}$ also caused strong dendrite degeneration in C4da neurons (fig. S4, A to D). These data indicate that the *Eato-RB* isoform is necessary for neuronal maintenance.

Next, to determine whether the long Eato protein isoform is sufficient for *Eato*'s function, we expressed *UAS-Eato(B)* in *Eato* KO animals. The gRNA target sequences in the *UAS-Eato(B)* coding

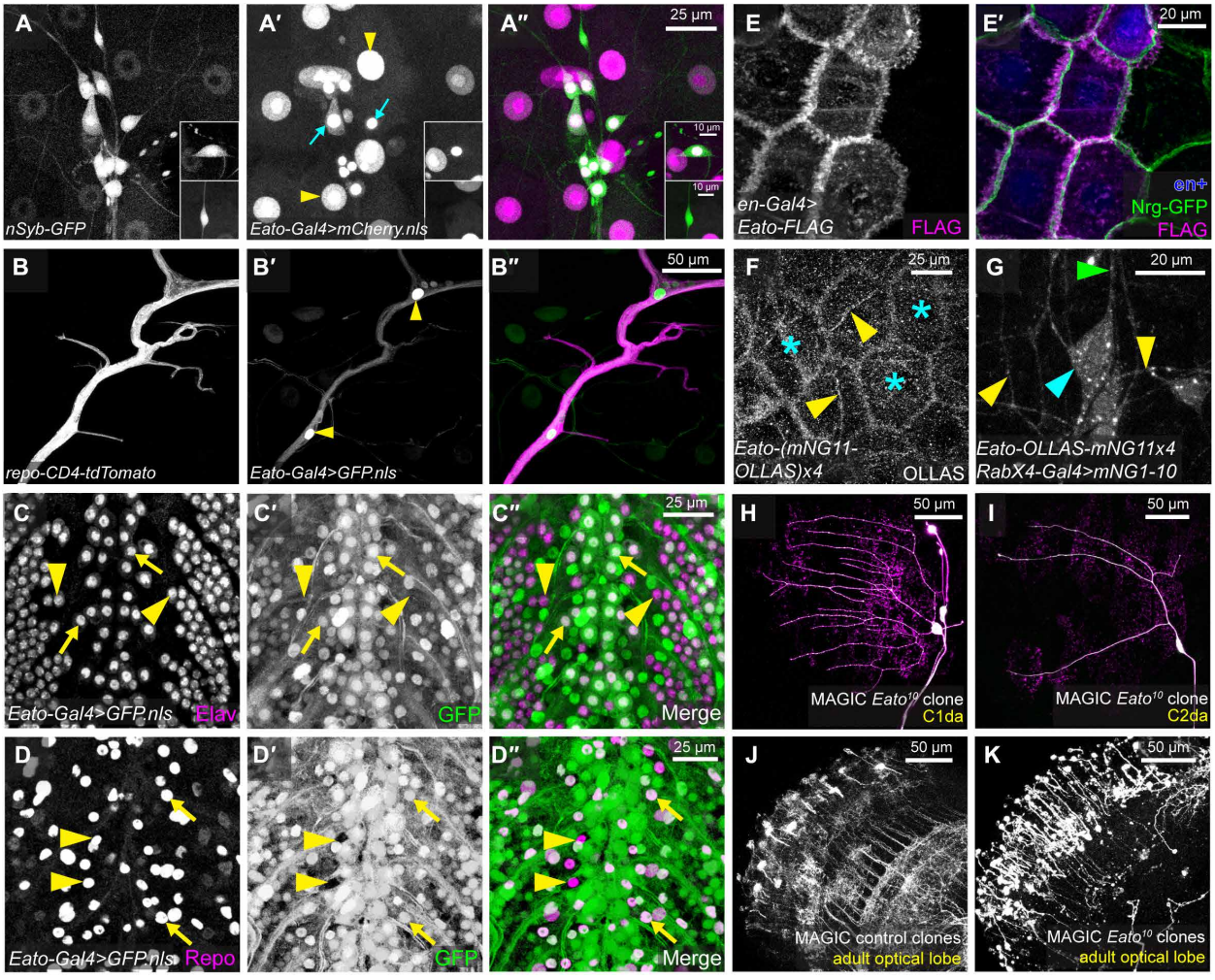

Fig. 4. *Eato* encodes a membrane protein required for the integrity of diverse neurons in both PNS and CNS. (**A** to **A**″) *Eato* expression on the larval body wall at 96 hours AEL. *nSyb-tdGFP* labels neurons (A). *Eato-Gal4*^{MI14571} drives expression of nuclear mCherry (A′). Yellow arrowheads: epidermal nuclei; blue arrows: neuronal nuclei. Top insets show a bd neuron expressing *Eato*, and bottom insets show an es neuron without *Eato* expression. (**B** to **B**″) *Eato* expression in an intersegmental nerve bundle. Glial cells are labeled by *repo-CD4-tdTomato* (B). *Eato-Gal4*^{MI14571} drives the expression of a nuclear GFP (B′). Yellow arrowheads: glial nuclei. (**C** to **D**″) *Eato* expression in the CNS. *Eato-Gal4*^{MI14571} drives the expression of a nuclear GFP. Elav staining visualizes neuronal nuclei [(C) to (C″)]. Arrows: neurons with *Eato* expression; arrowheads: neurons without *Eato* expression. Repo staining visualizes glial nuclei [(D) to (D″)]. Arrows: glia with *Eato* expression; arrowheads: glia without *Eato* expression. (**E** and **E**′) Localization of FLAG-tagged Eato protein in epidermal cells. Eato(B) is expressed by *en-Gal4* and detected by FLAG antibody staining. In (E′), mIFP shows the *en+* domain (blue), and Nrg-GFP shows cell junctions (green). (**F**) Endogenous Eato in *Eato-(mNG*$_{11}$*-OLLAS)×4*, detected by OLLAS staining. Yellow arrowheads: dendrite tracks; blue asterisks: epidermal cells. (**G**) Neuronal Eato in *Eato-(mNG*$_{11}$*-OLLAS)×4* homozygotes, detected by split-mNeonGreen reconstitution. mNG$_{1–10}$ is expressed by *RabX4-Gal4*. Cyan arrowhead: soma; green arrowhead: axon; yellow arrowheads: dendrites. (**H** and **I**) *Eato*^{10} homozygous clones in class I da (H) and class II da (I) neurons. Clones were labeled by *RabX4-Gal4 UAS-MApHS*. pHluorin is in green and tdTom is in magenta. Magenta-only signals indicate neuronal debris engulfed by epidermal cells. (**J** and **K**) Control (J) and *Eato*^{10} mutant (K) neuronal clones in the adult optical lobe. Clones were labeled by *RabX4-Gal4 UAS-MApHS*, but only tdTom signal is shown. MAGIC, mosaic analysis by gRNA-induced crossing-over.

sequence were altered by silent mutations to make the transgene gRNA-resistant. Eato(B) overexpression (OE) does not cause any dendrite phenotypes in WT neurons (fig. S4, E to H), and it completely prevented dendrite degeneration caused by *Eato* KO (Fig. 5, F to H, J, and K), demonstrating the sufficiency of the long isoform in maintaining neuronal integrity. Furthermore, to determine whether the putative ATPase activity of Eato is needed for its function, we mutated the key lysine (K) residue of the Walker A motif in each of the ATP-binding domains of Eato(B) into methionine (M). The resulting Eato(B.MM) mutant protein is predicted to be incapable of binding ATP and to lack transporter function (*33*, *55*). In contrast to *UAS-Eato(B)*, *UAS-Eato(B.MM)* failed to rescue *Eato* KO neurons (Fig. 5, I to K).

Last, to test whether Eato(B) can restore the phagocytic activity of *Eato*-deficient epidermal cells, we expressed Eato(B) in epidermal cells of whole-body *Eato* KO animals. The KO was achieved by using a ubiquitously expressed *tub-Cas9*, and Eato(B) expression was driven by *en-Gal4*, so that nonexpressing epidermal cells in the anterior hemisegment can serve as an internal control. These animals displayed dendrite degeneration specifically in the posterior hemisegment, as

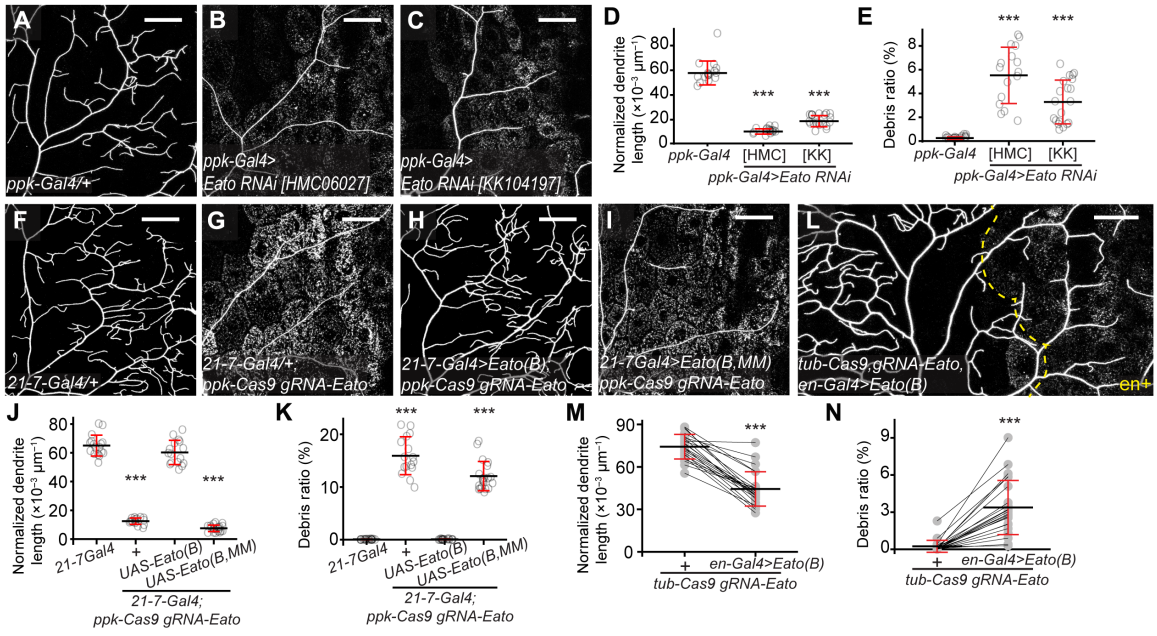

Fig. 5. Putative ABCA transporter activity is required for Eato's function. (**A** to **C**) Dendrites of C4da neurons in *ppk-Gal4* control (A), C4da-specific *Eato(B/C)* KD (B), and C4da-specific *Eato(B)* KD (C) late third-instar larvae. (**D** and **E**) Quantification of normalized dendrite length (D) and debris ratio (E) of neurons in (A) to (C). *n* = number of neurons and *N* = number of animals: *ppk-Gal4* (*n* = 16, *N* = 11); *ppk-Gal4>Eato-RNAi[HMC]* (*n* = 16, *N* = 14); *ppk-Gal4>Eato-RNAi[KK]* (*n* = 20, *N* = 13). The datasets of *ppk-Gal4* and *ppk-Gal4>Eato-RNAi[HMC06027]* are the same as in Fig. 1. (**F** to **K**) Dendrites of C4da neurons in *21-7-Gal4* control (F), C4da-specific *Eato* KO (G), C4da-specific *Eato* KO with da-specific *Eato(B)* OE (H), and C4da-specific *Eato* KO with da-specific *Eato(B.MM)* OE (I) late third-instar larvae. Normalized dendrite length is quantified in (J), and debris ratio is quantified in (K). *n* = number of neurons and *N* = number of animals: *21-7Gal4* (*n* = 16, *N* = 8); *21-7-Gal4 ppk-Cas9 gRNA-Eato* (*n* = 16, *N* = 8); *21-7-Gal4>UAS-Eato(B) ppk-Cas9 gRNA-Eato* (*n* = 17, *N* = 11); *21-7-Gal4>UAS-Eato(B,MM) ppk-Cas9 gRNA-Eato* (*n* = 20, *N* = 12). (**L**) Dendrites of C4da neurons in *en-Gal4 UAS-Eato(B); tub-Cas9 gRNA-Eato UAS-mIFP* animals. The *en+* domain is right to the yellow dashed line. The anterior nonexpressing region serves as a control. Comparisons between the control (+) and *en+* domains are shown in (**M**) (for normalized dendrite length) and (**N**) (for debris ratio). Data are from 23 neurons in 14 animals. *21-7-Gal4* drives expression in da neurons. C4da neurons were labeled by *ppk-MApHS* in (A) to (C), (F) to (I), and (L). Scale bars, 50 μm. In all plots, ***$P < 0.001$. [(D), (E), (J), and (K)] One-way ANOVA with Tukey post hoc test. [(M) and (N)] Paired *t* test.

indicated by the reduced dendrite density and the presence of dendrite debris (Fig. 5, L to N), suggesting successful rescue of epidermal phagocytic activity. As a comparison, Eato(B) OE in WT epidermal cells did not enable them to engulf WT dendrites (fig. S4, I to L). Together, the above data indicate that the full ABCA sequence of Eato is necessary and sufficient for its function in neurons and phagocytes and that the putative transporter activity is necessary for its function.

Eato prevents dendrite degeneration by antagonizing neuronal PS exposure

Given the role of PS exposure in inducing phagocytosis and the PS exposure observed on *Eato* KO neurons, we wondered whether the degeneration of *Eato*-deficient neurons is caused by PS exposure. To answer this question, we overexpressed *Drosophila* ATP8A in *Eato* KO neurons. ATP8A is a PS flippase in the P4-ATPase family and is responsible for keeping PS in the inner leaflet of the plasma membrane (*41*). Its OE can suppress PS exposure in both neurons and phagocytes (*28*, *41*). Neuronal expression of ATP8A completely suppressed the degeneration of *Eato* KO neurons (Fig. 6, A to D), suggesting that PS exposure is the cause of the degeneration. This result also suggests that Eato's normal function in neurons is to prevent PS exposure. We thus tested whether Eato(B) can antagonize ectopic PS exposure caused by disruptions of membrane lipid asymmetry. Ectopic PS exposure in C4da neurons can be induced by OE of the scramblase TMEM16F and simultaneous KO of *CDC50* (*27*), which encodes an obligatory chaperone for ATP8A (*56*). TMEM16F OE + *CDC50* KO neurons were associated with moderate levels of neuronal debris due to the ectopic PS exposure (Fig. 6, E and G) (*27*). However, additional Eato(B) expression in these neurons eliminated neuronal debris (Fig. 6, F and G). These results suggest that Eato normally suppresses PS exposure on neuronal surface to prevent neurites from being engulfed by phagocytes.

Epidermal Eato facilitates Drpr recruitment to degenerating dendrites

The engulfment receptor Drpr is normally found only at low levels on the plasma membrane of phagocytes, but it is recruited to the site of engulfment in response to PS exposure on the engulfment target (*41*, *57*). In the dendrite injury model, distinct Drpr staining overlapped with severed dendrites (fig. S5A), consistent with our previous results (*41*). The endogenous Eato (via OLLAS staining in the *Eato-OLLAS* allele) also accumulated along the same injured dendrites (fig. S5A). In contrast, neither Drpr nor Eato was enriched along uninjured dendrites (fig. S5A), suggesting that Eato and Drpr are corecruited specifically to injured dendrites. To further understand the engulfment defects of *Eato* LOF, we examined Drpr recruitment in *Eato*-deficient epidermal cells. As expected, Drpr was enriched along degenerating dendrites of *Eato* KO neurons on WT epidermal cells (Fig. 6, I to I″). However, the dendrite-overlapping Drpr staining was absent in whole-body *Eato* KO (Fig. 6, J to J″).

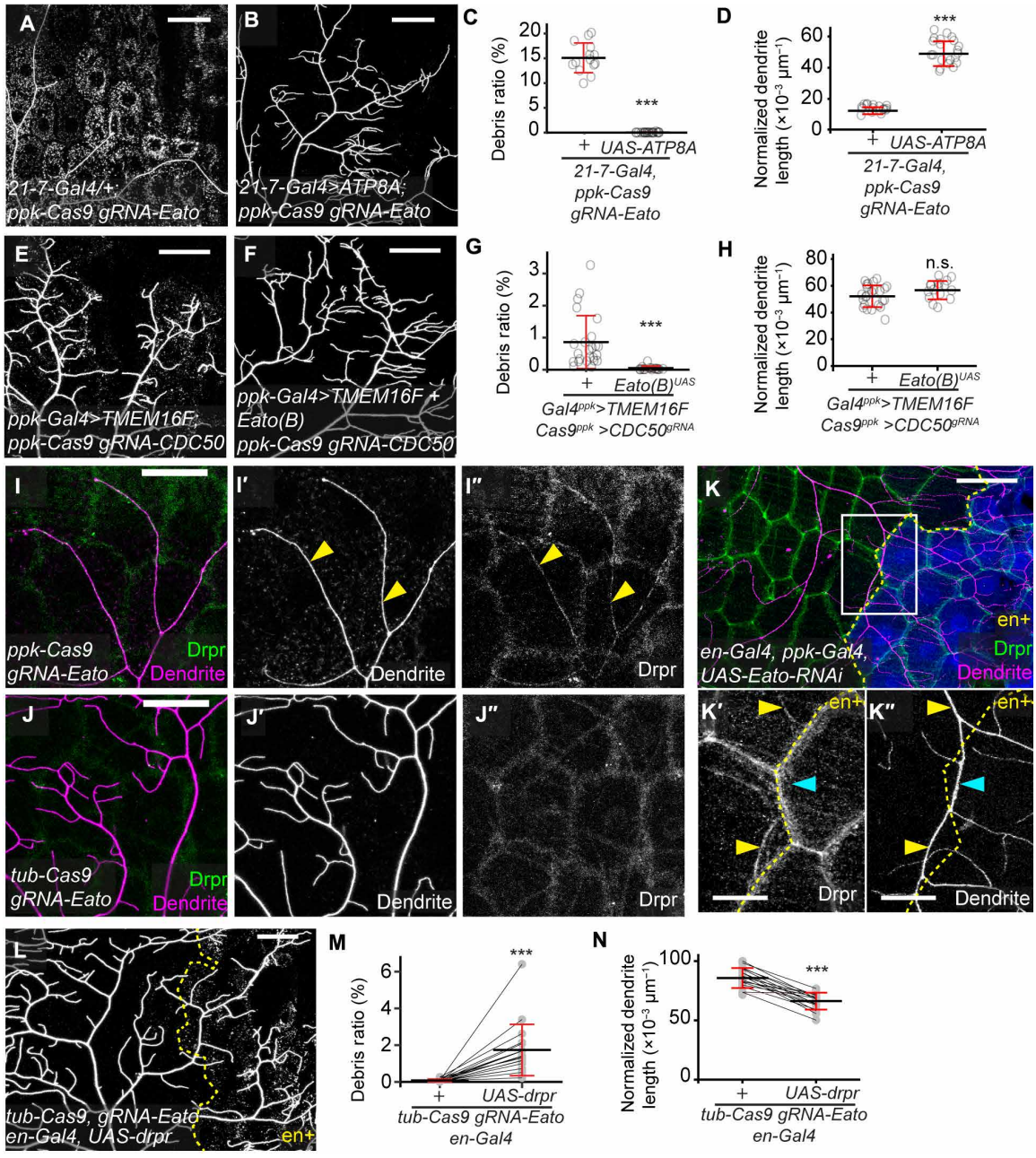

Fig. 6. Eato suppresses PS exposure in neurons and facilitates Drpr recruitment to degenerating dendrites in epidermal cells. (**A** to **D**) C4da-specific *Eato* KO (A) and C4da-specific *Eato* KO with da-specific ATP8A expression (B). Debris ratio is in (C), and normalized dendrite length is in (D). Sample sizes: *21-7-Gal4 ppk-Cas9 gRNA-Eato* ($n = 16$, $N = 8$); *21-7-Gal4 UAS-ATP8A ppk-Cas9 gRNA-Eato* ($n = 21$, $N = 11$). (**E** to **H**) C4da neuron dendrites with ectopic PS exposure (E) and additional Eato(B) OE (F). Ectopic PS exposure was induced by TMEM16F OE and simultaneous *CDC50* KO. Debris ratio is in (G), and normalized dendrite length is in (H). Sample sizes: $Gal4^{ppk}$>*TMEM16F* $Cas9^{ppk}$>$CDC50^{gRNA}$ ($n = 24$, $N = 14$); $Gal4^{ppk}$>*TMEM16F + Eato(B)* $Cas9^{ppk}$>$CDC50^{gRNA}$ ($n = 16$, $N = 12$). (**I** to **J**″) Drpr-GFP in C4da-specific *Eato* KO [(I) to (I″)] and whole-body *Eato* KO [(J) to (J″)] mid-third–instar larvae. Yellow arrowheads: Drpr-GFP alone dendrites. (**K** to **K**″) Drpr staining in a mid-third–instar larva where *Eato* is knocked down in both C4da neurons and the *en*+ domain. The *en*+ domain [mIFP, blue in (K)] is located right to the yellow dashed line in [(K′) and (K″)]. Yellow arrowheads: Drpr in control epidermal cells; cyan arrowheads: absence of Drpr in *Eato* KD epidermal cells. (**L**) Dendrites in whole-body *Eato* KO with Drpr OE by *en-Gal4*. The *en*+ region is right to the yellow dashed line. Debris ratio is in (**M**), and normalized dendrite length is in (**N**). Data are from 18 neurons in 11 animals. C4da neurons were labeled by *ppk-MApHS* in (A), (B), and (L); *ppk-CD4-tdTomato* in (E), (F), and (I) to (K″). Scale bars, 50 μm [(A), (B), (E), (F), and (I) to (L)] and 20 μm in [(K′) and (K″)]. ***$P < 0.001$. [(C), (D), (G), and (H)] Two-sample *t* test; [(M) and (N)] paired *t* test.

Considering that dendrites did not degenerate in whole-body *Eato* KO, the lack of Drpr accumulation on dendrites could be due to the absence of dendrite degeneration. To cause dendrites contacting *Eato*-deficient epidermal cells to degenerate, we knocked down *Eato* in both C4da neurons and *en*+ epidermal cells. In these animals, branches that straddle the border between WT and *Eato*-KD epidermal cells may undergo degeneration due to phagocytic attack by WT epidermal cells (Fig. 2, N and N′) and thus expose higher PS. We observed dendrite branches that traversed single *Eato*-KD cells (Fig. 6, K to K"). Drpr was recruited to the sites of the dendrites on WT (yellow arrowheads) but not *Eato*-KD (blue arrowheads) epidermal cells. Assuming that the level of PS exposure along the branch is relatively even, these results suggest that epidermal Eato acts upstream of Drpr recruitment. However, in older animals where *Eato*-KD dendrites degenerated even in the *en*+ domain, Drpr in *Eato*-KD epidermal cells was still recruited to the degenerating dendrites (fig. S5B), suggesting that *Eato* is not required for Drpr recruitment in epidermal cells.

Next, to test whether supplying more Drpr can compensate for the loss of *Eato* in epidermal cells, we overexpressed Drpr in *en*+ epidermal cells of whole-body *Eato* KO animals. The *en*+ domain showed increased debris levels and reduced dendrites as compared to the anterior control region (Fig. 6, L to N), indicating rescue of engulfment. Thus, Eato sensitizes phagocytes by facilitating Drpr recruitment, but more Drpr can compensate for the reduction of sensitivity caused by *Eato* deficiency.

Eato promotes engulfment activity of epidermal cells by suppressing PS exposure

Since Eato protects neurons by suppressing PS exposure on the cell surface, we wondered whether Eato also inhibits PS exposure on phagocytes. Thus, we knocked out *Eato* using *tub-Cas9* (*38*) and examined PS exposure on epidermal cells using GFP-Lact. We observed a moderate (3.39-fold) increase in GFP-Lact labeling as compared to the WT control (Fig. 7, A to C). Next, we asked whether *Eato* can suppress ectopic PS exposure on epidermal cells caused by flippase ablation. *CDC50* KO in epidermal cells resulted in strong labeling of GFP-Lact on the KO cells (Fig. 7D), consistent with CDC50/ATP8A being the primary PS flippase on the plasma membrane (*27*). Overexpressing Eato in *CDC50* KO epidermal cells reduced Lact-GFP labeling to 34.3% of the original level (Fig. 7, E and F), confirming that Eato is capable of reducing PS exposure on epidermal cell surfaces. Given that both ATP8A and Eato inhibit PS exposure on the cell surface, we wondered whether they genetically interact with each other. Eato-OLLAS staining showed 56 and 89% increases in epidermal KO of *CDC50* and *ATP8A* (fig. S6, A and B). On the other hand, the *ATP8A* mRNA level showed 61% increase in $Eato^{10}$ mutant larvae as measured by quantitative polymerase chain reaction (qPCR; fig. S6C). These results suggest that *ATP8A* and *Eato* are each up-regulated when the other is missing.

Is PS exposure on *Eato*-deficient epidermal cells responsible for the reduced phagocytosis? To answer this question, we coexpressed ATP8A and its chaperone CDC50 in *en*+ epidermal cells of whole-body *Eato* KO animals to suppress PS exposure. The *en*+ domain showed elevated debris levels (Fig. 7, G and H), suggesting partial restoration of engulfment activity. These data imply that PS exposure on phagocytes negatively affects phagocytosis. To test this idea directly, we ectopically induced PS exposure on epidermal cells by flippase KO and assayed the ability of epidermal cells to engulf degenerating dendrites. We first examined degenerating dendrites of *Eato*-KD neurons (Fig. 7I). Notably, simultaneous KO of the flippase chaperone *CDC50* in epidermal cells nearly completely suppressed the dendrite degeneration (Fig. 7, J, L, and M). Epidermal KO of *ATP8A* showed a similar, albeit milder, suppression of dendrite degeneration (Fig. 7, K to M). Next, we examined dendrite degeneration caused by neuronal expression of $TMEM16F^{CA}$ (Fig. 7N). Again, *CDC50* KO in epidermal cells suppressed this type of dendrite degeneration as effectively as epidermal KO of *drpr* and *Eato*, while epidermal KO of *ATP8A* caused a lightly milder suppression (Fig. 7, O to T). Together, the above results suggest that PS exposure on phagocytes inhibits sensing of PS on the engulfment target and that Eato promotes engulfment at least partially by suppressing PS exposure on phagocytes.

Lipid accumulation in cells is unlikely to account for the effects of *Eato* deficiency

Eato is thought to function as a floppase to export excessive lipids from *Drosophila* photoreceptors (*24*). In these neurons, ineffective clearance of lipid accumulation caused by oxidative stress speeds up neurodegeneration (*24*). To investigate whether lipid accumulation also contributes to the defects of *Eato*-deficient da neurons and epidermal cells, we first overexpressed Brummer (Bmm), a *Drosophila* triglyceride lipase, in *Eato* KO neurons. Bmm OE was previously shown to be effective in suppressing photoreceptor degeneration caused by lipid accumulation (*24*). However, we did not observe any rescue of dendrite degeneration by Bmm OE (fig. S6, D to G). Next, we used lipid storage droplet-2–enhanced green fluorescent protein (EGFP) to visualize lipid droplets, which store excessive neutral lipids, in neurons and epidermal cells. However, we did not observe detectable increases of lipid droplets in either tissue upon whole-body *Eato* KO (fig. S6, H to N). Although these results cannot completely exclude the possibility of lipid accumulation in *Eato*-deficient cells, they suggest that general lipid accumulation is not a major cause of the defects of *Eato*-deficient cells.

Human and *C. elegans* ABCA proteins can compensate for the loss of *Eato* in phagocytes

The human genome encodes 12 ABCA proteins involved in diverse biological processes (*4*). The *C. elegans* CED-7 is an ABCA protein involved in phagocytosis (*58*, *59*). To explore potential functional conservation between Eato and these homologs, we tested whether human and *C. elegans* ABCA genes can replace Eato's functions in epidermal cells and neurons. Toward this aim, we obtained *UAS-hABCA1* and *UAS-hABCA2* from the Bloomington *Drosophila* Stock Center and generated *UAS*-driven hABCA3, hABCA4, hABCA5, hABCA12, and CED-7 in our laboratory. We also made a *UAS-mouse ABCA7* (*mABCA7*) transgene. In the following tests, *UAS-Eato(B)* served as a positive control, while *UAS-Eato(B.MM)* served as a negative control; mammalian ABCA genes were expressed in flies at 29°C to facilitate protein folding.

To test rescue of *Eato* LOF in epidermal cells, we expressed ABCA genes in the *en*+ domain of whole-body *Eato* KO animals. Except mABCA7, all tested ABCA transgenes resulted in elevated levels of dendrite debris in the posterior hemisegment (Fig. 8, A to P), suggesting varying degrees of rescue. Among them, CED-7 rescued engulfment of dendrites as well as Eato(B), although its effects on dendrite reduction and debris level are more variable (Fig. 8, D, O, and P). The effects of human ABCA genes appear generally weaker than that of Eato(B) (Fig. 8, O and P). We next tested rescue of *Eato* LOF in neurons.

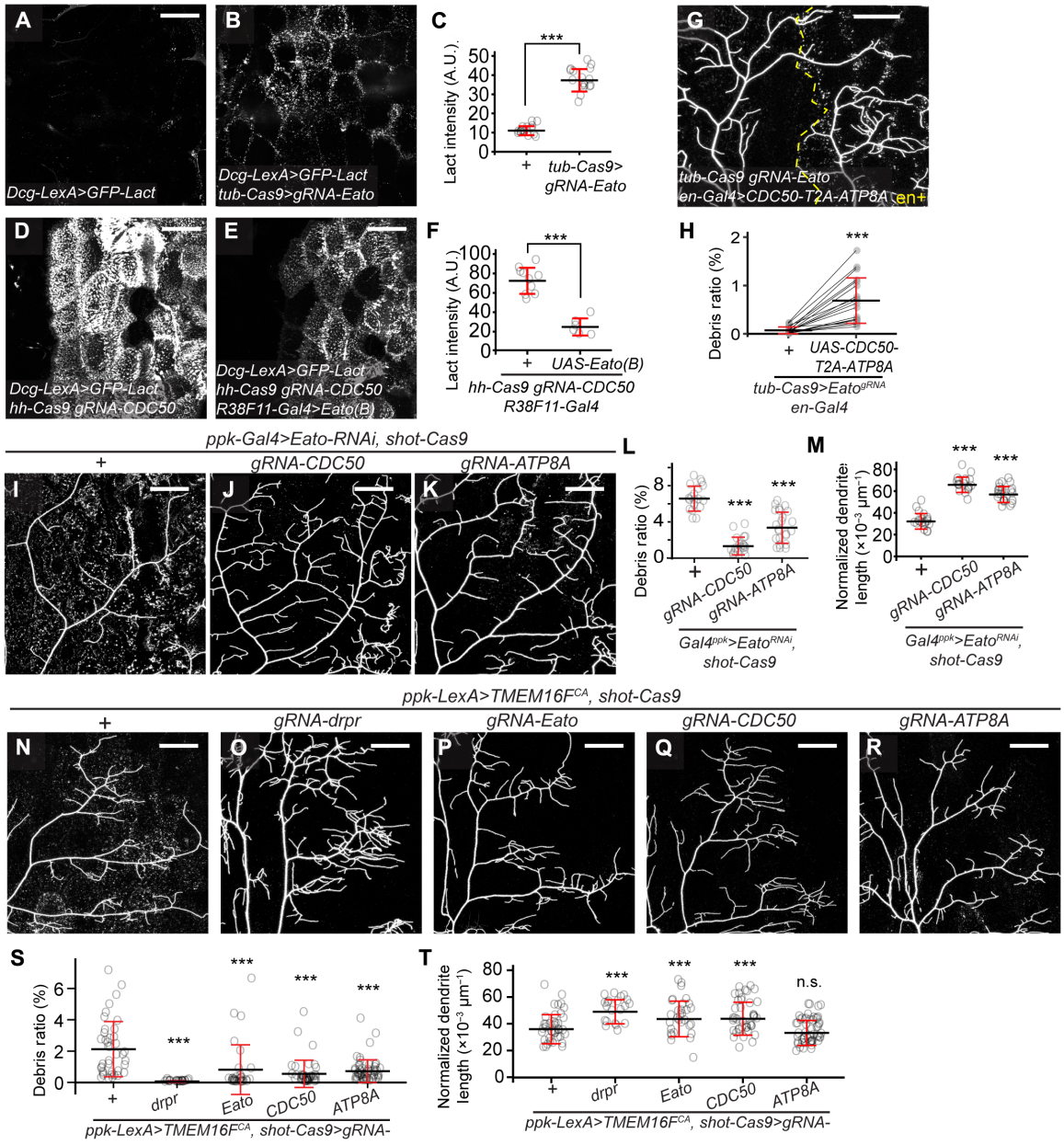

Fig. 7. *Eato* promotes engulfment activity of epidermal cells by suppressing PS exposure. (**A** to **C**) GFP-Lact on control (A) and *Eato* KO [(B), *tub-Cas9>gRNA-Eato*] epidermal cells. GFP intensity: (C). Sample sizes: + ($n = 16$, $N = 8$); *tub-Cas9>gRNA-Eato* ($n = 17$, $N = 11$). (**D** to **F**) GFP-Lact on *CDC50* KO [(D), by *hh-Cas9*] and *CDC50* KO with *Eato* OE (E) epidermal cells, at a lower brightness setting to avoid oversaturation. GFP intensity: (F). Sample sizes: *hh-Cas9 gRNA-CDC50 R38F11-Gal4* ($n = 10$, $N = 5$); *hh-Cas9 gRNA-CDC50 R38F11-Gal4 UAS-Eato(B)* ($n = 6$, $N = 4$). (**G** and **H**) Dendrites (G) and debris level (H) in whole-body *Eato* KO with *en-Gal4>CDC50-2A-ATP8A* (G). Nineteen neurons in 12 animals. (**I** to **M**) C4da-specific *Eato* KD (I) and additional *CDC50* KO (J) or *ATP8A* KO (K) in epidermal cells. Debris ratio: (L); normalized dendrite length: (M). Sample sizes: *Gal4^{ppk}>Eato^{RNAi} shot-Cas9* ($n = 19$, $N = 13$); *Gal4^{ppk}>Eato^{RNAi} shot-Cas9 gRNA-CDC50* ($n = 19$, $N = 13$); *Gal4^{ppk}>Eato^{RNAi} shot-Cas9 gRNA-ATP8A* ($n = 23$, $N = 14$). (**N** to **T**) Neuronal *TMEM16F^{CA}* OE (N) and additional *drpr* KO (O), *Eato* KO (P), *CDC50* KO (Q), or *ATP8A* KO (R) in epidermal cells. Debris ratio: (S); normalized dendrite length: (T). Sample sizes: *ppk-LexA>TMEM16F^{CA} shot-Cas9* ($n = 40$, $N = 19$); *ppk-LexA>TMEM16F^{CA} shot-Cas9 gRNA-drpr* ($n = 21$, $N = 15$); *ppk-LexA>TMEM16F^{CA} shot-Cas9 gRNA-Eato* ($n = 30$, $N = 15$); *ppk-LexA>TMEM16F^{CA} shot-Cas9 gRNA-CDC50* ($n = 41$, $N = 25$); *ppk-LexA>TMEM16F^{CA} shot-Cas9 gRNA-ATP8A* ($n = 54$, $N = 24$). The datasets in (N) to (P) are the same as in Fig. 2. C4da neurons were labeled by *ppk-MApHS*. Scale bars, 50 μm. ***$P < 0.001$. [(C) and (F)] *T* test; (H) paired *t* test; [(L), (M), (S), and (T)] one-way ANOVA with Tukey post hoc test.

However, none of the ABCA homologs obviously suppressed dendrite degeneration when expressed in *Eato*-KO C4da neurons, although some of them resulted in reduced debris levels (fig. S7). These data suggest that most of the ABCA proteins examined share some similar biochemical activity that can boost engulfment activity of phagocytes, but they do not seem to function the same way as Eato in neurons.

DISCUSSION

Eato plays opposing roles in neurons and phagocytes to control phagocytosis-driven neurite degeneration

In this study, we discovered that a single ABCA transporter, Eato, plays opposite roles on the defensive and the offensive sides of phagocytosis-driven neurodegeneration. On the defensive side, Eato

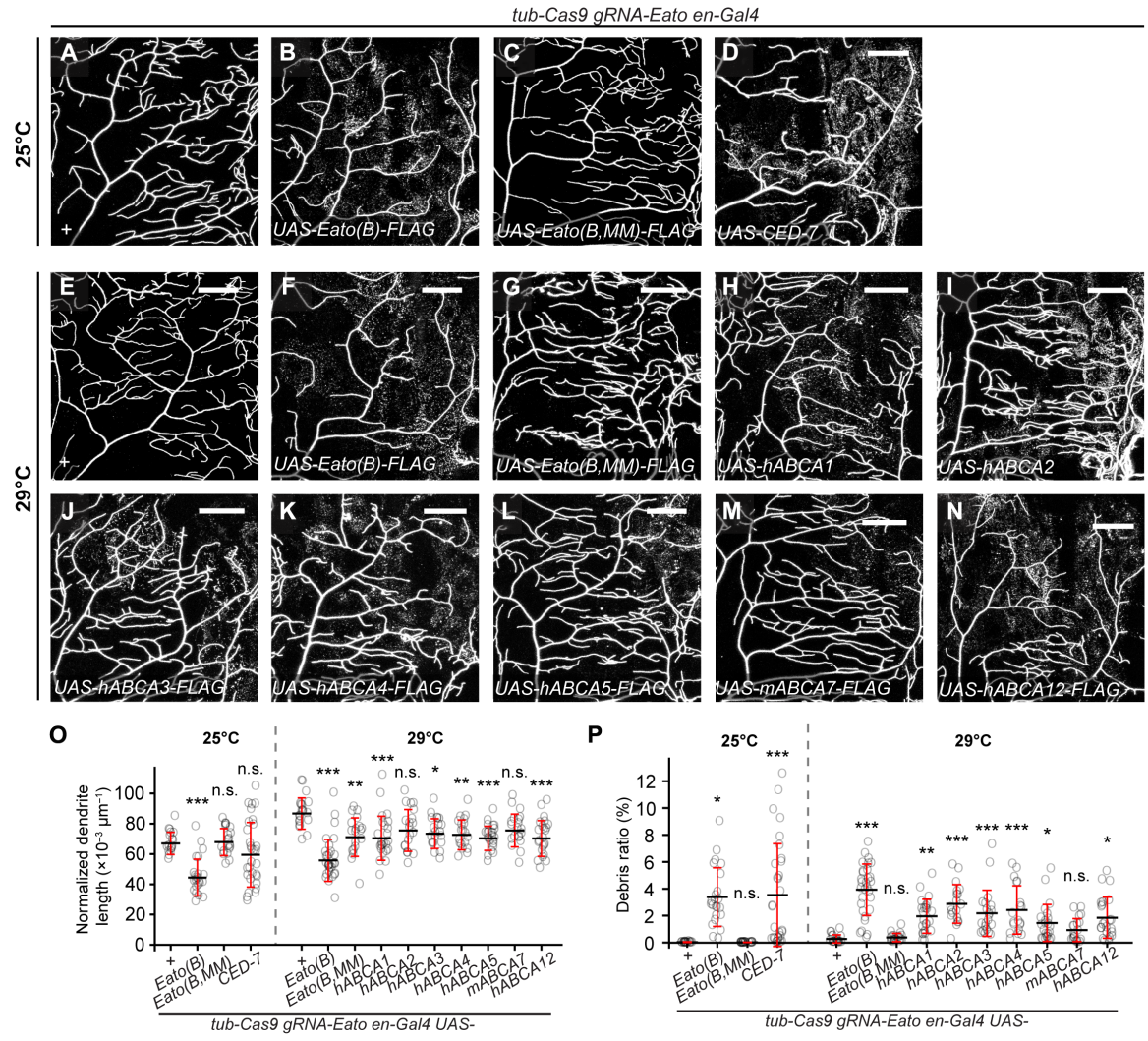

Fig. 8. Human and *C. elegans* ABCA proteins can compensate for the loss of *Eato* in phagocytes. (**A** to **D**) Dendrites of C4da neurons in whole-body *Eato* KO (A) and with additional OE of *Eato(B)* (B), *Eato(B.MM)* (C), and *CED-7* (D) in the *en*+ domain. The larvae were raised at 25°C. (**E** to **N**) Dendrites of C4da neurons in whole-body *Eato* KO (E) and with additional OE of *Eato(B)* (F), *Eato(B.MM)* (G), human *ABCA1* (H), human *ABCA2* (I), human *ABCA3* (J), human *ABCA4* (K), human *ABCA5* (L), mouse *ABCA7* (M), and human *ABCA12* (N) in the *en*+ domain. The larvae were raised at 29°C. (**O** and **P**) Quantification of normalized dendrite length (O) and debris ratio (P) in (A) to (N). *n* = number of neurons and *N* = number of animals. 25°C: + (*n* = 17, *N* = 10); *Eato(B)* (*n* = 23, *N* = 14); *Eato(B,MM)* (*n* = 20, *N* = 7); *CED-7* (*n* = 30, *N* = 11). 29°C: + (*n* = 20, *N* = 6); *Eato(B)* (*n* = 30, *N* = 13); *Eato(B,MM)* (*n* = 19, *N* = 6); *hABCA1* (*n* = 24, *N* = 7); *hABCA2* (*n* = 19, *N* = 6); *hABCA3* (*n* = 20, *N* = 6); *hABCA4* (*n* = 19, *N* = 6); *hABCA5* (*n* = 23, *N* = 5); *mABCA7* (*n* = 20, *N* = 6); *hABCA12* (*n* = 23, *N* = 7). Scale bars, 50 µm. In all plots, ***$P < 0.001$, **$P < 0.01$, and *$P < 0.05$; one-way ANOVA with Tukey post hoc test.

protects neurons from becoming targets of phagocytosis, but on the offensive side, Eato enhances the ability of phagocytes to detect nearby engulfment targets. Consequently, the loss of *Eato* in neurons alone causes surrounding phagocytes to attack and engulf the axons and dendrites, resulting in severe neurodegeneration. In contrast, removing *Eato* from both neurons and resident phagocytes prevents neurodegeneration because *Eato*-deficient phagocytes are no longer able to detect eat-me signals exposed on neurons. Eato's opposing roles in neurons and phagocytes are both related to its ability to suppress PS exposure on the cell surface, suggesting a common biochemical activity underlying both phenotypes. Although multiple ABCA genes are known to be involved in neurodegeneration in model organisms or implicated in neurodegenerative human diseases, to our knowledge, such dual roles for ABCA genes in neurodegeneration have never been reported. Thus, Eato's functions represent a unique mechanism by which ABCA genes are involved in neurodegeneration.

Our results show that Eato protects diverse neurons in both the PNS and the CNS, suggesting that Eato is required for a general biological process shared by many neuronal types. However, *Eato* deficiency in some neuronal types (e.g., motor neurons) did not seem to cause degeneration (fig. S3H). At least two possibilities might explain this neuronal diversity. First, another ABCA gene may play similar roles as *Eato* in these neurons, such that the loss of *Eato* produces no effects. Along this line, we found that although Eato is broadly expressed in the nervous system, its expression is absent in some neurons. *Eato* LOF is not expected to cause degeneration of those neurons. Second, different neurons may interact with surrounding

cells of different phagocytic capabilities, such that *Eato* mutant neurons are not engulfed if the neighboring cells are poor phagocytes. Supporting the idea of uneven phagocyte capacities, we found that epidermal cells are potent phagocytes that can eat most dendrites of live da neurons, while CNS glia cause only mild axon degeneration of da neurons on their own (Fig. 3).

Several ABCA genes, including *Eato*, are known to promote phagocytosis (*33*, *42*, *60*, *61*). Specifically, *Eato* is required for follicle cells to engulf dying nurse cells in the female germ line (*42*). Consistent with this finding, we found that *Eato* is also required for epidermal cells and glia to engulf dendrites and axons, respectively, of *Eato*-deficient da neurons. Considering that loss of neuronal *Eato* causes degeneration of diverse neurons while whole-animal *Eato* mutants show no signs of neurodegeneration, *Eato* must be widely required for phagocytes in the nervous system to engulf *Eato* mutant neurons. It was not previously known how Eato promotes phagocytosis. Using multiple models of dendrite degeneration, we show here that Eato is not required for engulfment per se; rather, it boosts the sensitivity of phagocytes toward PS-exposing targets. Eato does so by allowing for recruitment of the engulfment receptor Drpr to the site of engulfment, similar to the role of *C. elegans* CED-7 in recruitment of the Drpr homolog Ced-1 (*35*).

PS exposure is responsible for the defects of *Eato* deficiency in both neurons and phagocytes

Mechanistically, our results support the idea that Eato exerts its function in both neurons and phagocytes by suppressing PS exposure. In both tissues, OE of the PS-specific flippase ATP8A can rescue the defects caused by the loss of *Eato*, suggesting that surface PS exposure is necessary for these defects. Meanwhile, Eato OE suppresses dendrite loss caused by ectopic PS exposure in neurons and dramatically reduces PS exposure induced by flippase KO in epidermal cells, suggesting that Eato can reduce cell surface PS exposure. Thus, it appears that Eato carries out similar biochemical activities in both cell types, resulting in less cell surface PS.

How does Eato suppress PS exposure? Previous work has linked two ABCA genes with both PS exposure and phagocytosis. Murine *ABCA1* is required for efficient clearance of apoptotic cells in the developing limb bud and for the phagocytic activity of macrophages (*33*). Meanwhile, ABCA1 promotes Ca^{2+}-induced PS exposure in blood cells (*33*). In *C. elegans* embryos, *ced-7* is also required for efficient PS exposure on apoptotic cells (*35*). These observations are consistent with ABCA1 and CED-7 being lipid floppases that export lipids from the interior of cells. In contrast, the effect of Eato on PS exposure appears to be opposite to those of ABCA1 and CED-7 and is more similar to that of the flippase ATP8A. However, our results also show important distinctions between Eato and the PS flippase. On the one hand, flippase KO in epidermal cells results in high levels of PS exposure, whereas *Eato* KO produces a milder effect. On the other hand, *Eato* KO in neurons causes much more severe dendrite degeneration than flippase KO (*27*). Thus, unlike P4-ATPases that import PS across the lipid bilayer and maintain general PS asymmetry on the plasma membrane, Eato seems to specifically suppress certain potent eat-me signals related to PS. One possibility to reconcile these observations is that Eato may function to selectively clear a subset of PS lipids that are particularly potent in inducing phagocytosis from the cell surface. In vitro analysis of Eato's biochemical activity will be critical to establish how Eato regulates PS homeostasis at the plasma membrane.

How does PS exposure on phagocytes inhibit engulfment of PS-exposing dendrites? A simple hypothesis is that PS on the surface of phagocytes interacts with the engulfment receptor Drpr on the same membrane and thus interferes with Drpr's ability to interact with PS exposed on dendrites. This hypothesis predicts that increasing the PS level on dendrites may outcompete PS on phagocytes and restore engulfment. Injury is known to induce rapid and high PS exposure on severed dendrites (*27*, *28*), and these dendrites can still be engulfed by *Eato*-KO epidermal cells.

Eato was previously linked to neurodegeneration through its role in exporting excessive lipids from photoreceptors (*24*). In these cells, the loss of *Eato* results in accumulation of oxidized lipids inside lipid droplets, causing photoreceptors to die earlier in the presence of oxidative stress. However, we do not think a similar mechanism accounts for the neurodegeneration observed here. First, we did not detect lipid droplet increases in *Eato* mutant neurons. Second, reducing the lipid load inside neurons by lipase OE did not affect the degeneration of *Eato* mutant neurons. Third, the *Eato* mutant neurons we examined here degenerate much more rapidly (within 5 days) than *Eato*-deficient photoreceptors exposed to oxidative stress (>20 days). Last, in the retina, glial cells protect photoreceptors by taking up excessive lipids from photoreceptors rather than being responsible for neurodegeneration by engulfing photoreceptors (*23*). Thus, we posit that, outside the retina, Eato plays a much broader protective role in the nervous system by suppressing PS exposure.

Conserved and diverged functions of ABCA proteins

Besides human ABCA1 and CED-7, we found that several other ABCA proteins (hABCA2, hABCA3, hABCA4, hABCA5, and hABCA12) can rescue the phagocytic defects of *Eato* KO epidermal cells to various extents. These results are unexpected, considering that ABCA proteins do not necessarily have the same biochemical activities (*2*). For example, although most of the ABCA proteins characterized so far are involved in exporting lipids, ABCA4 is a flippase for *N*-retinylidene-phosphatidylethanolamine (*62*). However, our results suggest that many, if not all, ABCA proteins may have some shared biochemical properties that can enhance phagocytosis.

Considering that Eato's roles in neurons and phagocytes both involve suppression of PS exposure, it is further unexpected that, although several ABCA proteins can compensate for the loss of *Eato* in epidermal cells, none of them can rescue *Eato* mutant neurons. One possibility to account for this difference is that Eato may require additional, neuronal-specific factors to function properly in neurons, and these factors do not interact with ABCA proteins derived from humans and worms. Another possibility is that neurons require a more complete suppression of PS exposure than phagocytes to inhibit the effects of *Eato* LOF. A potential caveat of these rescue experiments is that the worm and human ABCA homologues may not be properly expressed or folded in *Drosophila* neurons, further contributing to the lack of rescues.

Axons and dendrites contribute differently to overall neuronal integrity

An interesting finding from our results is that phagocytic damage to dendrites affects the integrity of axons much more than the other way around: Blocking engulfment of dendrites largely rescued axon degeneration of *Eato* KO neurons, but suppressing axon engulfment had little effect on dendrite degeneration. These results suggest that dendrites contribute more to the overall health of neurons than

axons. One possible explanation is that axons may be more separated metabolically or spatially from the cell body than dendrites through cellular compartmentalization (*63*, *64*), such that injury signals initiated in axons do not spread effectively to the cell body. Alternatively, dendrites are more important to the overall health of da neurons because they occupy a larger cellular volume than axons.

Potential roles of ABCA genes in neurodegenerative diseases by regulating PS-mediated phagocytosis

Neuron-phagocyte interactions play important roles in the progress of neurodegeneration (*65*). Besides clearing dead neurons and debris of neurites, phagocytosis can promote or even drive neurodegeneration (*26*, *65*). For example, mutations in *Atp8a2* result in spontaneous axon degeneration and paralysis in mice, most likely due to phagocytosis of axons induced by ectopic PS exposure (*66*). We recently found that disruption of NAD^+ metabolism, which is common in neurodegenerative diseases (*67*, *68*), can cause neurons to lose neurites due to PS-induced phagocytosis (*28*). Here, we present another example where dysregulation of PS homeostasis on the plasma membrane results in phagocytosis-dependent neurodegeneration. Several human ABCA genes are associated with neurodegenerative diseases, including ABCA1, ABCA2, and ABCA7 in AD, ABCA5 in Parkinson's disease, and ABCA4 in macular degeneration (*5*, *6*, *69*, *70*). It is an intriguing question whether any human ABCA protein is neuroprotective by suppressing PS exposure on neurons, like Eato in *Drosophila*. However, to address this question, it is important to investigate neuronal-specific LOF of ABCA genes in in vivo mammalian models, since potential neurodegeneration could be phagocytosis dependent and the LOF of ABCA genes in phagocytes could suppress neurodegeneration.

MATERIALS AND METHODS

Drosophila strains

The fly strains used in this study are listed in table S1 (the Supplementary Materials). In general, C4da neurons were labeled by *ppk-MApHS*, *ppk-CD4-tdTom*, or *ppk-Gal4 UAS-CD4-tdTom*; PS exposure on cell surface was visualized by *dcg-Gal4 UAS-GFP-Lact* or *dcg-LexA LexAop-GFP-Lact*.

Molecular cloning and transgenic flies, generation of *Eato* KI, Gal4, and mutant flies, CRISPR-TRiM, mosaic analysis, live imaging, injury assay, dissection and staining, image analysis and quantification, statistical analysis are described in Supplementary Methods.

Supplementary Materials

This PDF file includes:

Supplementary Methods
Figs. S1 to S7
Tables S1
References

REFERENCES AND NOTES

1. M. Dean, K. Moitra, R. Allikmets, The human ATP-binding cassette (ABC) transporter superfamily. *Hum. Mutat.* **43**, 1162–1182 (2022).
2. F. Quazi, R. S. Molday, Lipid transport by mammalian ABC proteins. *Essays Biochem.* **50**, 265–290 (2011).
3. C. Broccardo, M.-F. Luciani, G. Chimini, The ABCA subclass of mammalian transporters. *Biochim. Biophys. Acta* **1461**, 395–404 (1999).
4. C. Albrecht, E. Viturro, The ABCA subfamily—gene and protein structures, functions and associated hereditary diseases. *Pflugers Arch.* **453**, 581–589 (2007).
5. A. P. Piehler, M. Ozcurumez, W. E. Kaminski, A-subclass ATP-binding cassette proteins in brain lipid homeostasis and neurodegeneration. *Front. Psych.* **3**, 17 (2012).
6. L. Bossaerts, R. Cacace, C. Van Broeckhoven, The role of ATP-binding cassette subfamily A in the etiology of Alzheimer's disease. *Mol. Neurodegener.* **17**, 31 (2022).
7. C. Bellenguez, F. Küçükali, I. E. Jansen, L. Kleineidam, S. Moreno-Grau, N. Amin, A. C. Naj, R. Campos-Martin, B. Grenier-Boley, V. Andrade, P. A. Holmans, A. Boland, V. Damotte, S. J. van der Lee, M. R. Costa, T. Kuulasmaa, Q. Yang, I. de Rojas, J. C. Bis, A. Yaqub, I. Prokic, J. Chapuis, S. Ahmad, V. Giedraitis, D. Aarsland, P. Garcia-Gonzalez, C. Abdelnour, E. Alarcón-Martín, D. Alcolea, M. Alegret, I. Alvarez, V. Álvarez, N. J. Armstrong, A. Tsolaki, C. Antúnez, I. Appollonio, M. Arcaro, S. Archetti, A. A. Pastor, B. Arosio, L. Athanasiu, H. Bailly, N. Banaj, M. Baquero, S. Barral, A. Beiser, A. B. Pastor, J. E. Below, P. Benchek, L. Benussi, C. Berr, C. Besse, V. Bessi, G. Binetti, A. Bizarro, R. Blesa, M. Boada, E. Boerwinkle, B. Borroni, S. Boschi, P. Bossù, G. Bråthen, J. Bressler, C. Bresner, H. Brodaty, K. J. Brookes, L. I. Brusco, D. Buiza-Rueda, K. Bûrger, V. Burholt, W. S. Bush, M. Calero, L. B. Cantwell, G. Chene, J. Chung, M. L. Cuccaro, Á. Carracedo, R. Cecchetti, L. Cervera-Carles, C. Charbonnier, H.-H. Chen, C. Chillotti, S. Ciccone, J. A. H. R. Claassen, C. Clark, E. Conti, A. Corma-Gómez, E. Costantini, C. Custodero, D. Daian, M. C. Dalmasso, A. Daniele, E. Dardiotis, J.-F. Dartigues, P. P. de Deyn, K. de Paiva Lopes, L. D. de Witte, S. Debette, J. Deckert, T. del Ser, N. Denning, A. De Stefano, M. Dichgans, J. Diehl-Schmid, M. Diez-Fairen, P. D. Rossi, S. Djurovic, E. Duron, E. Düzel, C. Dufouil, G. Eiriksdottir, S. Engelborghs, V. Escott-Price, A. Espinosa, M. Ewers, K. M. Faber, T. Fabrizio, S. F. Nielsen, D. W. Fardo, L. Farotti, C. Fenoglio, M. Fernández-Fuertes, R. Ferrari, C. B. Ferreira, E. Ferri, B. Fin, P. Fischer, T. Fladby, K. Fließbach, B. Fongang, M. Fornage, J. Fortea, T. M. Foroud, S. Fostinelli, N. C. Fox, E. Franco-Macías, M. J. Bullido, A. Frank-García, L. Froelich, B. Fulton-Howard, D. Galimberti, J. M. García-Alberca, P. García-González, S. Garcia-Madrona, G. Garcia-Ribas, R. Ghidoni, I. Giegling, G. Giorgio, A. M. Goate, O. Goldhardt, D. Gomez-Fonseca, A. González-Pérez, C. Graff, G. Grande, E. Green, T. Grimmer, E. Grünblatt, M. Grunin, V. Gudnason, T. Guetta-Baranes, A. Haapasalo, G. Hadjigeorgiou, J. L. Haines, K. L. Hamilton-Nelson, H. Hampel, O. Hanon, J. Hardy, A. M. Hartmann, L. Hausner, J. Harwood, S. Heilmann-Heimbach, S. Helisalmi, M. T. Heneka, I. Hernández, M. J. Herrmann, P. Hoffmann, C. Holmes, H. Holstege, R. H. Vilas, M. Hulsman, J. Humphrey, G. J. Biessels, X. Jian, C. Johansson, G. R. Jun, Y. Kastumata, J. Kauwe, P. G. Kehoe, L. Kilander, A. K. Ståhlbom, M. Kivipelto, A. Koivisto, J. Kornhuber, M. H. Kosmidis, W. A. Kukull, P. P. Kuksa, B. W. Kunkle, A. B. Kuzma, C. Lage, E. J. Laukka, L. Launer, A. Lauria, C.-Y. Lee, J. Lehtisalo, O. Lerch, A. Lleó, W. Longstreth Jr., O. Lopez, A. L. de Munain, S. Love, M. Löwemark, L. Luckcuck, K. L. Lunetta, Y. Ma, J. Macías, C. A. Mac Leod, W. Maier, F. Mangialasche, M. Spallazzi, M. Marquié, R. Marshall, E. R. Martin, A. M. Montes, C. M. Rodríguez, C. Masullo, R. Mayeux, S. Mead, P. Mecocci, M. Medina, A. Meggy, S. Mehrabian, S. Mendoza, M. Menéndez-González, P. Mir, S. Moebus, M. Mol, L. Molina-Porcel, L. Montrreal, L. Morelli, F. Moreno, K. Morgan, T. Mosley, M. M. Nöthen, C. Muchnik, S. Mukherjee, B. Nacmias, T. Ngandu, G. Nicolas, B. G. Nordestgaard, R. Olaso, A. Orellana, M. Orsini, G. Ortega, A. Padovani, C. Paolo, G. Papenberg, L. Parnetti, F. Pasquier, P. Pastor, G. Peloso, A. Pérez-Cordón, J. Pérez-Tur, P. Pericard, O. Peters, Y. A. L. Pijnenburg, J. A. Pineda, G. Piñol-Ripoll, C. Pisanu, T. Polak, J. Popp, D. Posthuma, J. Priller, R. Puerta, O. Quenez, I. Quintela, J. Q. Thomassen, A. Rábano, I. Rainero, F. Rajabli, I. Ramakers, L. M. Real, M. J. T. Reinders, C. Reitz, D. Reyes-Dumeyer, P. Ridge, S. Riedel-Heller, P. Riederer, N. Roberto, E. Rodriguez-Rodriguez, A. Rongve, I. R. Allende, M. Rosende-Roca, J. L. Royo, E. Rubino, D. Rujescu, M. E. Sáez, P. Sakka, I. Saltvedt, Á. Sanabria, M. B. Sánchez-Arjona, F. Sanchez-Garcia, P. S. Juan, R. Sánchez-Valle, S. B. Sando, C. Sarnowski, C. L. Satizabal, M. Scamosci, N. Scarmeas, E. Scarpini, P. Scheltens, N. Scherbaum, M. Scherer, M. Schmid, A. Schneider, J. M. Schott, G. Selbæk, D. Seripa, M. Serrano, J. Sha, A. A. Shadrin, O. Skrobot, S. Slifer, G. J. L. Snijders, H. Soininen, V. Solfrizzi, A. Solomon, Y. Song, S. Sorbi, O. Sotolongo-Grau, G. Spalletta, A. Spottke, A. Squassina, E. Stordal, J. P. Tartan, L. Tárraga, N. Tesí, A. Thalamuthu, T. Thomas, G. Tosto, L. Traykov, L. Tremolizzo, A. Tybjærg-Hansen, A. Uitterlinden, A. Ullgren, I. Ulstein, S. Valero, O. Valladares, C. Van Broeckhoven, J. Vance, B. N. Vardarajan, A. van der Lugt, J. Van Dongen, J. van Rooij, J. van Swieten, R. Vandenberghe, F. Verhey, J.-S. Vidal, J. Vogelgsang, M. Vyhnalek, M. Wagner, D. Wallon, L.-S. Wang, R. Wang, L. Weinhold, J. Wiltfang, G. Windle, B. Woods, M. Yannakoulia, H. Zare, Y. Zhao, X. Zhang, C. Zhu, M. Zulaica, EADB, GR@ACE, DEGESCO, EADI, GERAD, Demgene, FinnGen, ADGC, CHARGE, L. A. Farrer, B. M. Psaty, M. Ghanbari, T. Raj, P. Sachdev, K. Mather, F. Jessen, M. A. Ikram, A. de Mendonça, J. Hort, M. Tsolaki, M. A. Pericak-Vance, P. Amouyel, J. Williams, R. Frikke-Schmidt, J. Clarimon, J.-F. Deleuze, G. Rossi, S. Seshadri, O. A. Andreassen, M. Ingelsson, M. Hiltunen, K. Sleegers, G. D. Schellenberg, C. M. van Duijn, R. Sims, W. M. van der Flier, A. Ruiz, A. Ramirez, J.-C. Lambert, New insights into the genetic etiology of Alzheimer's disease and related dementias. *Nat. Genet.* **54**, 412–436 (2022).
8. P. Hollingworth, D. Harold, R. Sims, A. Gerrish, J.-C. Lambert, M. M. Carrasquillo, R. Abraham, M. L. Hamshere, J. S. Pahwa, V. Moskvina, K. Dowzell, N. Jones, A. Stretton, C. Thomas, A. Richards, D. Ivanov, C. Widdowson, J. Chapman, S. Lovestone, J. Powell, P. Proitsi, M. K. Lupton, C. Brayne, D. C. Rubinsztein, M. Gill, B. Lawlor, A. Lynch, K. S. Brown, P. A. Passmore, D. Craig, B. M. Guinness, S. Todd, C. Holmes, D. Mann, A. D. Smith,

H. Beaumont, D. Warden, G. Wilcock, S. Love, P. G. Kehoe, N. M. Hooper, E. R. L. C. Vardy, J. Hardy, S. Mead, N. C. Fox, M. Rossor, J. Collinge, W. Maier, F. Jessen, E. Rüther, B. Schürmann, R. Heun, H. Kölsch, H. van den Bussche, I. Heuser, J. Kornhuber, J. Wiltfang, M. Dichgans, L. Frölich, H. Hampel, J. Gallacher, M. Hüll, D. Rujescu, I. Giegling, A. M. Goate, J. S. K. Kauwe, C. Cruchaga, P. Nowotny, J. C. Morris, K. Mayo, K. Sleegers, K. Bettens, S. Engelborghs, P. P. De Deyn, C. Van Broeckhoven, G. Livingston, N. J. Bass, H. Gurling, A. M. Quillin, R. Gwilliam, P. Deloukas, A. Al-Chalabi, C. E. Shaw, M. Tsolaki, A. B. Singleton, R. Guerreiro, T. W. Mühleisen, M. M. Nöthen, S. Moebus, K.-H. Jöckel, N. Klopp, H.-E. Wichmann, V. S. Pankratz, S. B. Sando, J. O. Aasly, M. Barcikowska, Z. K. Wszolek, D. W. Dickson, N. R. Graff-Radford, R. C. Petersen, the Alzheimer's Disease Neuroimaging Initiative, C. M. van Duijn, M. M. B. Breteler, M. A. Ikram, A. L. De Stefano, A. L. Fitzpatrick, O. Lopez, L. J. Launer, S. Seshadri, CHARGE consortium, C. Berr, D. Campion, J. Epelbaum, J.-F. Dartigues, C. Tzourio, A. Alpérovitch, M. Lathrop, EADI1 consortium, T. M. Feulner, P. Friedrich, C. Riehle, M. Krawczak, S. Schreiber, M. Mayhaus, S. Nicolhaus, S. Wagenpfeil, S. Steinberg, H. Stefansson, K. Stefansson, J. Snædal, S. Björnsson, P. V. Jonsson, V. Chouraki, B. Genier-Boley, M. Hiltunen, H. Soininen, O. Combarros, D. Zelenika, M. Delepine, M. J. Bullido, F. Pasquier, I. Mateo, A. Frank-Garcia, E. Porcellini, O. Hanon, E. Coto, V. Alvarez, P. Bosco, G. Siciliano, M. Mancuso, F. Panza, V. Solfrizzi, B. Nacmias, S. Sorbi, P. Bossù, P. Piccardi, B. Arosio, G. Annoni, D. Seripa, A. Pilotto, E. Scarpini, D. Galimberti, A. Brice, D. Hannequin, F. Licastro, L. Jones, P. A. Holmans, T. Jonsson, M. Riemenschneider, K. Morgan, S. G. Younkin, M. J. Owen, M. O'Donovan, P. Amouyel, J. Williams, Common variants at *ABCA7, MS4A6A/MS4A4E, EPHA1, CD33* and *CD2AP* are associated with Alzheimer's disease. *Nat. Genet.* **43**, 429–435 (2011).

9. T. M. Do, M. Ouellet, F. Calon, G. Chimini, H. Chacun, R. Farinotti, F. Bourasset, Direct evidence of abca1-mediated efflux of cholesterol at the mouse blood-brain barrier. *Mol. Cell. Biochem.* **357**, 397–404 (2011).
10. W. S. Kim, A. S. Rahmanto, A. Kamili, K.-A. Rye, G. J. Guillemin, I. C. Gelissen, W. Jessup, A. F. Hill, B. Garner, Role of ABCG1 and ABCA1 in regulation of neuronal cholesterol efflux to apolipoprotein E discs and suppression of amyloid-β peptide generation. *J. Biol. Chem.* **282**, 2851–2861 (2007).
11. S. E. Wahrle, H. Jiang, M. Parsadanian, J. Legleiter, X. Han, J. D. Fryer, T. Kowalewski, D. M. Holtzman, ABCA1 is required for normal central nervous system ApoE levels and for lipidation of astrocyte-secreted apoE. *J. Biol. Chem.* **279**, 40987–40993 (2004).
12. Y. Y. Cho, O.-H. Kwon, S. Chung, Preferred Endocytosis of Amyloid Precursor Protein from Cholesterol-Enriched Lipid Raft Microdomains. *Molecules* **25**, 5490 (2020).
13. K. J. Anstey, K. Ashby-Mitchell, R. Peters, Updating the evidence on the association between serum cholesterol and risk of late-life dementia: Review and meta-analysis. *J. Alzheimers Dis.* **56**, 215–228 (2017).
14. T. Tokuda, M. Calero, E. Matsubara, R. Vidal, A. Kumar, B. Permanne, B. Zlokovic, J. D. Smith, M. J. Ladu, A. Rostagno, B. Frangione, J. Ghiso, Lipidation of apolipoprotein E influences its isoform-specific interaction with Alzheimer's amyloid beta peptides. *Biochem. J.* **348**, 359–365 (2000).
15. J. Zhao, M. D. Davis, Y. A. Martens, M. Shinohara, N. R. Graff-Radford, S. G. Younkin, Z. K. Wszolek, T. Kanekiyo, G. Bu, *APOE* ε4/ε4 diminishes neurotrophic function of human iPSC-derived astrocytes. *Hum. Mol. Genet.* **26**, 2690–2700 (2017).
16. K. Satoh, S. Abe-Dohmae, S. Yokoyama, P. St George-Hyslop, P. E. Fraser, ATP-binding cassette transporter A7 (ABCA7) loss of function alters Alzheimer amyloid processing. *J. Biol. Chem.* **290**, 24152–24165 (2015).
17. N. Sakae, C.-C. Liu, M. Shinohara, J. Frisch-Daiello, L. Ma, Y. Yamazaki, M. Tachibana, L. Younkin, A. Kurti, M. M. Carrasquillo, F. Zou, D. Sevlever, G. Bisceglio, M. Gan, R. Fol, P. Knight, M. Wang, X. Han, J. D. Fryer, M. L. Fitzgerald, Y. Ohyagi, S. G. Younkin, G. Bu, T. Kanekiyo, ABCA7 deficiency accelerates amyloid-β generation and Alzheimer's neuronal pathology. *J. Neurosci.* **36**, 3848–3859 (2016).
18. Y. Fu, J.-H. T. Hsiao, G. Paxinos, G. M. Halliday, W. S. Kim, ABCA7 mediates phagocytic clearance of amyloid-β in the brain. *J. Alzheimers Dis.* **54**, 569–584 (2016).
19. W. S. Kim, H. Li, K. Ruberu, S. Chan, D. A. Elliott, J. K. Low, D. Cheng, T. Karl, B. Garner, Deletion of *Abca7* increases cerebral amyloid-β accumulation in the J20 mouse model of Alzheimer's disease. *J. Neurosci.* **33**, 4387–4394 (2013).
20. H. Sun, R. S. Molday, J. Nathans, Retinal stimulates ATP hydrolysis by purified and reconstituted ABCR, the photoreceptor-specific ATP-binding cassette transporter responsible for Stargardt disease. *J. Biol. Chem.* **274**, 8269–8281 (1999).
21. J. Weng, N. L. Mata, S. M. Azarian, R. T. Tzekov, D. G. Birch, G. H. Travis, Insights into the function of Rim protein in photoreceptors and etiology of Stargardt's disease from the phenotype in *abcr* knockout mice. *Cell* **98**, 13–23 (1999).
22. T. L. Lenis, J. Hu, S. Y. Ng, Z. Jiang, S. Sarfare, M. B. Lloyd, N. J. Esposito, W. Samuel, C. Jaworski, D. Bok, S. C. Finnemann, M. J. Radeke, T. M. Redmond, G. H. Travis, R. A. Radu, Expression of ABCA4 in the retinal pigment epithelium and its implications for Stargardt macular degeneration. *Proc. Natl. Acad. Sci. U.S.A.* **115**, E11120–E11127 (2018).
23. L. Liu, K. Zhang, H. Sandoval, S. Yamamoto, M. Jaiswal, E. Sanz, Z. Li, J. Hui, B. H. Graham, A. Quintana, H. J. Bellen, Glial lipid droplets and ROS induced by mitochondrial defects promote neurodegeneration. *Cell* **160**, 177–190 (2015).
24. M. J. Moulton, S. Barish, I. Ralhan, J. Chang, L. D. Goodman, J. G. Harland, P. C. Marcogliese, J. O. Johansson, M. S. Ioannou, H. J. Bellen, Neuronal ROS-induced glial lipid droplet formation is altered by loss of Alzheimer's disease-associated genes. *Proc. Natl. Acad. Sci. U.S.A.* **118**, e2112095118 (2021).
25. K. Segawa, S. Nagata, An Apoptotic 'eat me' signal: Phosphatidylserine exposure. *Trends Cell Biol.* **25**, 639–650 (2015).
26. M. L. Sapar, C. Han, Die in pieces: How *Drosophila* sheds light on neurite degeneration and clearance. *J. Genet. Genomics* **46**, 187–199 (2019).
27. M. L. Sapar, H. Ji, B. Wang, A. R. Poe, K. Dubey, X. Ren, J. Q. Ni, C. Han, Phosphatidylserine externalization results from and causes neurite degeneration in *Drosophila*. *Cell Rep.* **24**, 2273–2286 (2018).
28. H. Ji, M. L. Sapar, A. Sarkar, B. Wang, C. Han, Phagocytosis and self-destruction break down dendrites of *Drosophila* sensory neurons at distinct steps of Wallerian degeneration. *Proc. Natl. Acad. Sci. U.S.A.* **119**, e2204683119 (2022).
29. K. Segawa, S. Kurata, Y. Yanagihashi, T. R. Brummelkamp, F. Matsuda, S. Nagata, Caspase-mediated cleavage of phospholipid flippase for apoptotic phosphatidylserine exposure. *Science* **344**, 1164–1168 (2014).
30. J. Suzuki, M. Umeda, P. J. Sims, S. Nagata, Calcium-dependent phospholipid scrambling by TMEM16F. *Nature* **468**, 834–838 (2010).
31. T. Fujii, A. Sakata, S. Nishimura, K. Eto, S. Nagata, TMEM16F is required for phosphatidylserine exposure and microparticle release in activated mouse platelets. *Proc. Natl. Acad. Sci. U.S.A.* **112**, 12800–12805 (2015).
32. J. Suzuki, D. P. Denning, E. Imanishi, H. R. Horvitz, S. Nagata, Xk-related protein 8 and CED-8 promote phosphatidylserine exposure in apoptotic cells. *Science* **341**, 403–406 (2013).
33. Y. Hamon, C. Broccardo, O. Chambenoit, M. F. Luciani, F. Toti, S. Chaslin, J. M. Freyssinet, P. F. Devaux, J. McNeish, D. Marguet, G. Chimini, ABC1 promotes engulfment of apoptotic cells and transbilayer redistribution of phosphatidylserine. *Nat. Cell Biol.* **2**, 399–406 (2000).
34. J. Mapes, Y. Z. Chen, A. Kim, S. Mitani, B. H. Kang, D. Xue, CED-1, CED-7, and TTR-52 regulate surface phosphatidylserine expression on apoptotic and phagocytic cells. *Curr. Biol.* **22**, 1267–1275 (2012).
35. V. Venegas, Z. Zhou, Two alternative mechanisms that regulate the presentation of apoptotic cell engulfment signal in *Caenorhabditis elegans*. *Mol. Biol. Cell* **18**, 3180–3192 (2007).
36. Y. Zhang, H. Wang, E. Kage-Nakadai, S. Mitani, X. Wang, *C. elegans* secreted lipid-binding protein NRF-5 mediates PS appearance on phagocytes for cell corpse engulfment. *Curr. Biol.* **22**, 1276–1284 (2012).
37. M. C. Phillips, Is ABCA1 a lipid transfer protein? *J. Lipid Res.* **59**, 749–763 (2018).
38. A. R. Poe, B. Wang, M. L. Sapar, H. Ji, K. Li, T. Onabajo, R. Fazliyeva, M. Gibbs, Y. Qiu, Y. Hu, C. Han, Robust CRISPR/Cas9-mediated tissue-specific mutagenesis reveals gene redundancy and perdurance in *Drosophila*. *Genetics* **211**, 459–472 (2019).
39. W. B. Grueber, L. Y. Jan, Y. N. Jan, Tiling of the *Drosophila* epidermis by multidendritic sensory neurons. *Development* **129**, 2867–2878 (2002).
40. C. Han, Y. Song, H. Xiao, D. Wang, N. C. Franc, L. Y. Jan, Y. N. Jan, Epidermal cells are the primary phagocytes in the fragmentation and clearance of degenerating dendrites in *Drosophila*. *Neuron* **81**, 544–560 (2014).
41. H. Ji, B. Wang, Y. Shen, D. Labib, J. Lei, X. Chen, M. Sapar, A. Boulanger, J. M. Dura, C. Han, The *Drosophila* chemokine-like Orion bridges phosphatidylserine and Draper in phagocytosis of neurons. *Proc. Natl. Acad. Sci. U.S.A.* **120**, e2303392120 (2023).
42. C. S. Santoso, T. L. Meehan, J. S. Peterson, T. M. Cedano, C. V. Turlo, K. McCall, The ABC transporter *Eato* promotes cell clearance in the *Drosophila melanogaster* ovary. *G3 (Bethesda)* **8**, 833–843 (2018).
43. T. Le, Z. Jia, S. C. Le, Y. Zhang, J. Chen, H. Yang, An inner activation gate controls TMEM16F phospholipid scrambling. *Nat. Commun.* **10**, 1846 (2019).
44. Y. E. Kim, J. Chen, J. R. Chan, R. Langen, Engineering a polarity-sensitive biosensor for time-lapse imaging of apoptotic processes and degeneration. *Nat. Methods* **7**, 67–73 (2010).
45. V. Shacham-Silverberg, H. Sar Shalom, R. Goldner, Y. Golan-Vaishenker, N. Gurwicz, I. Gokhman, A. Yaron, Phosphatidylserine is a marker for axonal debris engulfment but its exposure can be decoupled from degeneration. *Cell Death Dis.* **9**, 1116 (2018).
46. M. R. Freeman, *Drosophila* central nervous system Glia. *Cold Spring Harb. Perspect. Biol.* **7**, a020552 (2015).
47. K. J. Venken, K. L. Schulze, N. A. Haelterman, H. Pan, Y. He, M. Evans-Holm, J. W. Carlson, R. W. Levis, A. C. Spradling, R. A. Hoskins, H. J. Bellen, MiMIC: A highly versatile transposon insertion resource for engineering *Drosophila melanogaster* genes. *Nat. Methods* **8**, 737–743 (2011).
48. F. Diao, H. Ironfield, H. Luan, F. Diao, W. C. Shropshire, J. Ewer, E. Marr, C. J. Potter, M. Landgraf, B. H. White, Plug-and-play genetic access to *Drosophila* cell types using exchangeable exon cassettes. *Cell Rep.* **10**, 1410–1421 (2015).
49. G. T. Koreman, Y. Xu, Q. Hu, Z. Zhang, S. E. Allen, M. F. Wolfner, B. Wang, C. Han, Upgraded CRISPR/Cas9 tools for tissue-specific mutagenesis in *Drosophila*. *Proc. Natl. Acad. Sci. U.S.A.* **118**, e2014255118 (2021).

50. S. Feng, S. Sekine, V. Pessino, H. Li, M. D. Leonetti, B. Huang, Improved split fluorescent proteins for endogenous protein labeling. *Nat. Commun.* **8**, 370 (2017).
51. S. H. Park, C. Cheong, J. Idoyaga, J. Y. Kim, J. H. Choi, Y. Do, H. Lee, J. H. Jo, Y. S. Oh, W. Im, R. M. Steinman, C. G. Park, Generation and application of new rat monoclonal antibodies against synthetic FLAG and OLLAS tags for improved immunodetection. *J. Immunol. Methods* **331**, 27–38 (2008).
52. O. Riabinina, D. Luginbuhl, E. Marr, S. Liu, M. N. Wu, L. Luo, C. J. Potter, Improved and expanded Q-system reagents for genetic manipulations. *Nat. Methods* **12**, 219–222 (2015).
53. S. E. Allen, G. T. Koreman, A. Sarkar, B. Wang, M. F. Wolfner, C. Han, Versatile CRISPR/Cas9-mediated mosaic analysis by gRNA-induced crossing-over for unmodified genomes. *PLoS Biol.* **19**, e3001061 (2021).
54. W. Song, M. Onishi, L. Y. Jan, Y. N. Jan, Peripheral multidendritic sensory neurons are necessary for rhythmic locomotion behavior in *Drosophila* larvae. *Proc. Natl. Acad. Sci. U.S.A.* **104**, 5199–5204 (2007).
55. M. P. Anderson, M. J. Welsh, Regulation by ATP and ADP of CFTR chloride channels that contain mutant nucleotide-binding domains. *Science* **257**, 1701–1704 (1992).
56. K. Tanaka, K. Fujimura-Kamada, T. Yamamoto, Functions of phospholipid flippases. *J. Biochem.* **149**, 131–143 (2011).
57. J. M. MacDonald, M. G. Beach, E. Porpiglia, A. E. Sheehan, R. J. Watts, M. R. Freeman, The *Drosophila* cell corpse engulfment receptor Draper mediates glial clearance of severed axons. *Neuron* **50**, 869–881 (2006).
58. R. E. Ellis, D. M. Jacobson, H. R. Horvitz, Genes required for the engulfment of cell corpses during programmed cell death in *Caenorhabditis elegans*. *Genetics* **129**, 79–94 (1991).
59. Z. Zhou, E. Hartwieg, H. R. Horvitz, CED-1 is a transmembrane receptor that mediates cell corpse engulfment in *C. elegans*. *Cell* **104**, 43–56 (2001).
60. N. Iwamoto, S. Abe-Dohmae, R. Sato, S. Yokoyama, ABCA7 expression is regulated by cellular cholesterol through the SREBP2 pathway and associated with phagocytosis. *J. Lipid Res.* **47**, 1915–1927 (2006).
61. Y. C. Wu, H. R. Horvitz, The *C. elegans* cell corpse engulfment gene *ced*-7 encodes a protein similar to ABC transporters. *Cell* **93**, 951–960 (1998).
62. F. Quazi, S. Lenevich, R. S. Molday, ABCA4 is an *N*-retinylidene-phosphatidylethanolamine and phosphatidylethanolamine importer. *Nat. Commun.* **3**, 925 (2012).
63. C. Glock, A. Biever, G. Tushev, B. Nassim-Assir, A. Kao, I. Bartnik, S. Tom Dieck, E. M. Schuman, The translatome of neuronal cell bodies, dendrites, and axons. *Proc. Natl. Acad. Sci. U.S.A.* **118**, e2113929118 (2021).
64. C. C. Overly, H. I. Rieff, P. J. Hollenbeck, Organelle motility and metabolism in axons vs dendrites of cultured hippocampal neurons. *J. Cell Sci.* **109** (Pt. 5), 971–980 (1996).
65. C. A. Butler, A. S. Popescu, E. J. A. Kitchener, D. H. Allendorf, M. Puigdellivol, G. C. Brown, Microglial phagocytosis of neurons in neurodegeneration, and its regulation. *J. Neurochem.* **158**, 621–639 (2021).
66. X. Zhu, R. T. Libby, W. N. de Vries, R. S. Smith, D. L. Wright, R. T. Bronson, K. L. Seburn, S. W. John, Mutations in a P-type ATPase gene cause axonal degeneration. *PLOS Genet.* **8**, e1002853 (2012).
67. E. Verdin, NAD^+ in aging, metabolism, and neurodegeneration. *Science* **350**, 1208–1213 (2015).
68. E. F. Fang, S. Lautrup, Y. Hou, T. G. Demarest, D. L. Croteau, M. P. Mattson, V. A. Bohr, NAD^+ in aging: Molecular mechanisms and translational implications. *Trends Mol. Med.* **23**, 899–916 (2017).
69. Y. Fu, J. H. Hsiao, G. Paxinos, G. M. Halliday, W. S. Kim, ABCA5 regulates amyloid-β peptide production and is associated with Alzheimer's disease neuropathology. *J. Alzheimers Dis.* **43**, 857–869 (2015).
70. W. S. Kim, G. M. Halliday, Changes in sphingomyelin level affect alpha-synuclein and ABCA5 expression. *J. Parkinsons Dis.* **2**, 41–46 (2012).
71. C. Han, L. Y. Jan, Y. N. Jan, Enhancer-driven membrane markers for analysis of nonautonomous mechanisms reveal neuron-glia interactions in *Drosophila*. *Proc. Natl. Acad. Sci. U.S.A.* **108**, 9673–9678 (2011).
72. K. J. Venken, Y. He, R. A. Hoskins, H. J. Bellen, P[acman]: A BAC transgenic platform for targeted insertion of large DNA fragments in *D. melanogaster*. *Science* **314**, 1747–1751 (2006).
73. A. R. Poe, L. Tang, B. Wang, Y. Li, M. L. Sapar, C. Han, Dendritic space-filling requires a neuronal type-specific extracellular permissive signal in *Drosophila*. *Proc. Natl. Acad. Sci. U.S.A.* **114**, E8062–E8071 (2017).
74. T. P. Newsome, B. Asling, B. J. Dickson, Analysis of *Drosophila* photoreceptor axon guidance in eye-specific mosaics. *Development* **127**, 851–860 (2000).
75. J. Garcia-Marques, I. Espinosa-Medina, K.-Y. Ku, C.-P. Yang, M. Koyama, H.-H. Yu, T. Lee, A programmable sequence of reporters for lineage analysis. *Nat. Neurosci.* **23**, 1618–1628 (2020).
76. T. Y. Belenkaya, C. Han, D. Yan, R. J. Opoka, M. Khodoun, H. Liu, X. Lin, *Drosophila* Dpp morphogen movement is independent of dynamin-mediated endocytosis but regulated by the glypican members of heparan sulfate proteoglycans. *Cell* **119**, 231–244 (2004).
77. C. Han, D. Wang, P. Soba, S. Zhu, X. Lin, L. Y. Jan, Y. N. Jan, Integrins regulate repulsion-mediated dendritic patterning of *Drosophila* sensory neurons by restricting dendrites in a 2D space. *Neuron* **73**, 64–78 (2012).
78. J. M. Suh, X. Gao, J. McKay, R. McKay, Z. Salo, J. M. Graff, Hedgehog signaling plays a conserved role in inhibiting fat formation. *Cell Metab.* **3**, 25–34 (2006).
79. S. Karuparti, A. T. Yeung, B. Wang, P. F. Guicardi, C. Han, A toolkit for converting Gal4 into LexA and Flippase transgenes in *Drosophila*. *G3 (Bethesda)* **13**, jkad003 (2023).
80. M. R. Freeman, J. Delrow, J. Kim, E. Johnson, C. Q. Doe, Unwrapping glial biology: Gcm target genes regulating glial development, diversification, and function. *Neuron* **38**, 567–580 (2003).

Acknowledgments: We thank H. Yang (Duke University), R. Allikmets (Columbia University), D. Xue (University of Colorado Boulder), Y. Hamon, G. Chimini (Aix Marseille University), and *Drosophila* Genomics Resource Center (DGRC) for plasmids; M. Freeman (Vollum Institute) and Developmental Studies Hybridoma Bank for antibodies; S.-B. Qian and X. Liu (Cornell University) for qPCR guidance and reagents; H. Ji (Stanford University) for dendrite ablation imaging and guidance; B. White (National Institute of Mental Health), M. Welte (University of Rochester), and Bloomington *Drosophila* Stock Center for fly stocks; Cornell BRC Imaging facility for access to microscopes (funded by NIH grant S10OD018516); Cornell CSCU for advice on statistics; M. Goldberg, J. Baskin, Q. Yuan, and members of the Han lab for feedback on the manuscript. **Funding:** This work was supported by NIH R01NS099125 (C.H.), NIH R24OD031953 (C.H.), and a Multi Investigator Seed Grant from Cornell University (C.H). **Author contributions:** Conceptualization: X.C. and C.H.; methodology: X.C. and C.H.; software: X.C.; validation: X.C., A.S., N.V.R., and C.H.; formal analysis: X.C., N.V.R., and R.C.; investigation: X.C., A.S., Z.H., N.V.R., and A.Y.; resources: B.W. and C.H.; writing—original draft: X.C. and C.H.; writing—review and editing: X.C., C.H., N.V.R., and A.T.Y.; visualization: X.C. and C.H.; supervision: C.H.; funding acquisition: C.H. **Competing interests:** The authors declare that they have no competing interests. **Data and materials availability:** All data needed to evaluate the conclusions in the paper are present in the paper and/or the Supplementary Materials.

Submitted 5 July 2024
Accepted 3 February 2025
Published 12 March 2025
10.1126/sciadv.adr5448